Two-fluid 20-moment simulation of fast magnetic reconnection

E. Alec Johnson

Department of Mathematics
KU Leuven

These slides were presented in my behalf at CSE13 in Boston Massachusetts on February 25, 2013

Abstract. *The 20-moment two-fluid-Maxwell model resolves diagonal pressure tensor components near the X-point when compared with Vlasov simulations of fast magnetic reconnection, in contrast to the 10-moment model. This occurs because, unlike the hyperbolic 10-moment model, the 20-moment model admits heat flux, which is a modeling requirement to admit steady-state 2D symmetric (driven) magnetic reconnection.*

Outline

Standard of truth: 2-species kinetic-Maxwell (classical)

- **Maxwell's equations:**

$$\partial_t \mathbf{B} + \nabla \times \mathbf{E} = 0,$$
$$\partial_t \mathbf{E} - c^2 \nabla \times \mathbf{B} = -\mathbf{J}/\epsilon,$$
$$\nabla \cdot \mathbf{B} = 0, \quad \nabla \cdot \mathbf{E} = \sigma/\epsilon.$$

- **Charge moments:**

$$\sigma := \sum_{\mathrm{s}} \frac{q_{\mathrm{s}}}{m_{\mathrm{s}}} \int f_{\mathrm{s}}\, d\mathbf{v},$$
$$\mathbf{J} := \sum_{\mathrm{s}} \frac{q_{\mathrm{s}}}{m_{\mathrm{s}}} \int \mathbf{v} f_{\mathrm{s}}\, d\mathbf{v}.$$

- **Kinetic equations:**

$$\begin{aligned} \partial_t f_{\mathrm{i}} + \mathbf{v} \cdot \nabla_{\mathbf{x}} f_i + \mathbf{a}_{\mathrm{i}} \cdot \nabla_{\mathbf{v}} f_{\mathrm{i}} &= \mathcal{C}_{\mathrm{i}} \\ \partial_t f_{\mathrm{e}} + \mathbf{v} \cdot \nabla_{\mathbf{x}} f_e + \mathbf{a}_{\mathrm{e}} \cdot \nabla_{\mathbf{v}} f_{\mathrm{e}} &= \mathcal{C}_{\mathrm{e}} \end{aligned}$$

- **Lorentz acceleration:**

$$\mathbf{a}_{\mathrm{i}} = \frac{q_i}{m_i} \left(\mathbf{E} + \mathbf{v} \times \mathbf{B} \right),$$
$$\mathbf{a}_{\mathrm{e}} = \frac{q_e}{m_e} \left(\mathbf{E} + \mathbf{v} \times \mathbf{B} \right).$$

BGK collision operator

$$\mathcal{C}_{\mathrm{s}} = \frac{f_\theta - f_{\mathrm{s}}}{\tau_{\mathrm{s}}},$$

where

$$f_\theta = \frac{\rho}{(2\pi\theta)^{3/2}} \exp\left(\frac{-|\mathbf{c}|^2}{2\theta} \right),$$
$$\theta := \langle |\mathbf{c}|^2/2 \rangle.$$

Fluid approximation requires a numerical collision operator

Fluid models are kinetic equation solvers.

- Characteristic speeds correspond to discrete velocities.
- Fluid models evolve moments.
- Moments define a representation F_s selected from a finite-dimensional space $\mathcal{F}$.
- convergence $F_s \to f_s$ requires an infinite number of moments.
- $\mathcal{F}$ is a good representation space when $\mathcal{C}$ is large but bad when $\mathcal{C}$ is small.

How can we justify fluid models when physically $\mathcal{C}_s = 0$?

- by a multiscale framework:
- fluid models are a coarse-scale model used to accelerate convergence of the lowest moments of the kinetic equation.
- $\mathcal{C}_s$ can be physically defined to incorporate all microscale effects not resolved by the coarse-scale model.
- in code, $\mathcal{C}_s \neq 0$ is a numerical mechanism to regularize f_s.
- collision period τ_s selects the largest time scale for resolution of velocity-space detail.

How to choose $\mathcal{C}_s$?

- use a simple choice based on what you want to resolve.
- BGK damps all components and moments representing perturbation from Maxwellian at the same rate τ_s^{-1}.
- Damping individual moments at tunable rates allows smooth transition to a model with more moments.
- Faster damping for higher moments corresponds to faster damping for finer-scale components of f_s.

Conserved Moment Evolution

Convention: *Products and powers of vectors are defined by tensor products.*

Conserved moments are moments of monomials in $\mathbf{v}$. Let $\chi = \chi(\mathbf{v})$. Take the χth moment of the kinetic equation:

$$\int_{\mathbf{v}} \chi \left(\partial_t f + \nabla_{\mathbf{x}} \cdot (\mathbf{v} f) + \nabla_{\mathbf{v}} \cdot (\mathbf{a} f) = \mathcal{C} \right)$$

Integrate by parts to get

$$\partial_t \int_{\mathbf{v}} \chi f + \nabla \cdot \int_{\mathbf{v}} \mathbf{v} \chi f = \int_{\mathbf{v}} f \mathbf{a} \cdot \nabla_{\mathbf{v}} \chi + \int_{\mathbf{v}} \chi \mathcal{C} \tag{1}$$

Choose $\chi = \mathbf{v}^n$. Define

$$\widetilde{\mathbf{F}}^n := \int_{\mathbf{v}} \mathbf{v}^n f, \qquad \widetilde{\mathbf{C}}^n := \int_{\mathbf{v}} \mathbf{v}^n \mathcal{C}.$$

Since $\mathbf{a} = \frac{q}{m}(\mathbf{E} + \mathbf{v} \times \mathbf{B})$,

$$\mathbf{a} \cdot \nabla_{\mathbf{v}} (\mathbf{v}^n) \overset{\vee}{=} \frac{q}{m} n \left(\mathbf{E} \mathbf{v}^{n-1} + \mathbf{v}^n \times \mathbf{B} \right).$$

Substituting into equation (1) gives:

General conserved moment evolution

$$\boxed{\partial_t \widetilde{\mathbf{F}}^n + \nabla \cdot \widetilde{\mathbf{F}}^{n+1} \overset{\vee}{=} \frac{q}{m} n \left(\mathbf{E} \widetilde{\mathbf{F}}^{n-1} + \widetilde{\mathbf{F}}^n \times \mathbf{B} \right) + \widetilde{\mathbf{C}}^n}$$

This is a hierarchy of moment evolution equations:

$$\begin{aligned}
&\partial_t \widetilde{\mathbf{F}}^0 + \nabla \cdot \widetilde{\mathbf{F}}^1 = \widetilde{\mathbf{C}}^0, \\
&\partial_t \widetilde{\mathbf{F}}^1 + \nabla \cdot \widetilde{\mathbf{F}}^2 = \frac{q}{m} (\mathbf{E} \widetilde{\mathbf{F}}^0 + \widetilde{\mathbf{F}}^1 \times \mathbf{B}) + \widetilde{\mathbf{C}}^1, \\
&\partial_t \widetilde{\mathbf{F}}^2 + \nabla \cdot \widetilde{\mathbf{F}}^3 \overset{\vee}{=} \frac{q}{m} 2 \left(\mathbf{E} \widetilde{\mathbf{F}}^1 + \widetilde{\mathbf{F}}^2 \times \mathbf{B} \right) + \widetilde{\mathbf{C}}^2, \\
&\partial_t \widetilde{\mathbf{F}}^3 + \nabla \cdot \widetilde{\mathbf{F}}^4 \overset{\vee}{=} \frac{q}{m} 3 \left(\mathbf{E} \widetilde{\mathbf{F}}^2 + \widetilde{\mathbf{F}}^3 \times \mathbf{B} \right) + \widetilde{\mathbf{C}}^3, \\
&\partial_t \widetilde{\mathbf{F}}^4 + \nabla \cdot \widetilde{\mathbf{F}}^5 \overset{\vee}{=} \frac{q}{m} 4 \left(\mathbf{E} \widetilde{\mathbf{F}}^3 + \widetilde{\mathbf{F}}^4 \times \mathbf{B} \right) + \widetilde{\mathbf{C}}^4.
\end{aligned}$$

Tensor notation:

- $\mathbf{AB} = \mathbf{A} \otimes \mathbf{B}$ = *tensor product,*
- Sym $\mathbf{A}$ = *symmetrization of tensor* $\mathbf{A}$*,*
- $\mathbf{A} \overset{\vee}{} \mathbf{B} = \text{Sym}(\mathbf{A} \otimes \mathbf{B})$*, and*
- $\mathbf{A} \overset{\vee}{=} \mathbf{B} \iff \text{Sym}\, \mathbf{A} = \text{Sym}\, \mathbf{B}$.

Primitive moments

- **Fluid closures should be Galilean invariant.**
  The kinetic equation is Galilean-invariant, so we require fluid closures to be Galilean-invariant.
- **Primitive moments are Galilean-invariant**

  Definitions:

  $$\rho = \int_v f$$

  $$\langle \chi \rangle := \frac{\int_{\mathbf{v}} \chi}{\rho}$$

  $$\mathbf{u} := \langle \mathbf{v} \rangle$$

  $$\mathbf{c} := \mathbf{v} - \mathbf{u}$$

  $$\mathbf{F}^n := \int_{\mathbf{v}} \mathbf{c}^n f$$

  Specifying closure in terms of primitive moments $\mathbf{F}^n$ ensures that closures are Galilean-invariant.

Mapping from conserved to primitive variables

To express primitive moments in terms of conserved moments we observe that

$$\mathbf{c}^n \overset{\vee}{=} (\mathbf{v}-\mathbf{u})^n \overset{\vee}{=} \sum_{j=0}^{n} (-1)^j \binom{n}{j} \mathbf{u}^j \mathbf{v}^{n-j}.$$

Multiplying by $\mathcal{C}$ and integrating over velocity,

$$\mathbf{C}^0 = \widetilde{\mathbf{C}}^0,$$
$$\mathbf{C}^1 = \widetilde{\mathbf{C}}^1 - \mathbf{u}\widetilde{\mathbf{C}}^0,$$
$$\mathbf{C}^2 = \widetilde{\mathbf{C}}^2 - 2\mathbf{u}\widetilde{\mathbf{C}}^1 + \mathbf{u}^2\widetilde{\mathbf{C}}^0,$$
$$\mathbf{C}^3 \overset{\vee}{=} \widetilde{\mathbf{C}}^3 - 3\mathbf{u}\widetilde{\mathbf{C}}^2 + 3\mathbf{u}^2\widetilde{\mathbf{C}}^1 - \mathbf{u}^3\widetilde{\mathbf{C}}^0,$$
$$\mathbf{C}^4 \overset{\vee}{=} \widetilde{\mathbf{C}}^4 - 4\mathbf{u}\widetilde{\mathbf{C}}^3 + 6\mathbf{u}^2\widetilde{\mathbf{C}}^2 - 4\mathbf{u}^3\widetilde{\mathbf{C}}^1 + \mathbf{u}^4\widetilde{\mathbf{C}}^0,$$

where in the absence of production $\widetilde{\mathbf{C}}^0 = 0$ and in the further absence of interspecies friction $\widetilde{\mathbf{C}}^1 = 0$.

Multiplying by f and integrating over velocity,

$$\mathbf{F}^0 = \rho,$$
$$\mathbf{F}^1 = \mathbf{0},$$
$$\mathbf{F}^2 = \widetilde{\mathbf{F}}^2 - \rho\mathbf{u}^2,$$
$$\mathbf{F}^3 \overset{\vee}{=} \widetilde{\mathbf{F}}^3 - 3\mathbf{u}\widetilde{\mathbf{F}}^2 + 2\rho\mathbf{u}^3,$$
$$\mathbf{F}^4 \overset{\vee}{=} \widetilde{\mathbf{F}}^4 - 4\mathbf{u}\widetilde{\mathbf{F}}^3 + 6\mathbf{u}^2\widetilde{\mathbf{F}}^2 - 3\rho\mathbf{u}^4,$$
$$\mathbf{F}^5 \overset{\vee}{=} \widetilde{\mathbf{F}}^5 - 5\mathbf{u}\widetilde{\mathbf{F}}^4 + 10\mathbf{u}^2\widetilde{\mathbf{F}}^3 - 10\mathbf{u}^3\widetilde{\mathbf{F}}^2 + 4\rho\mathbf{u}^5,$$

where we have used that $\widetilde{\mathbf{F}}^1 = \rho\mathbf{u}$.

In practice, when computing with conserved variables, we compute the primitive variables that we need for the closing moment and then use one of the relations

$$\widetilde{\mathbf{F}}^3 \overset{\vee}{=} \mathbf{F}^3 + 3\mathbf{u}\widetilde{\mathbf{F}}^2 - 2\rho\mathbf{u}^3,$$
$$\widetilde{\mathbf{F}}^4 \overset{\vee}{=} \mathbf{F}^4 + 4\mathbf{u}\widetilde{\mathbf{F}}^3 - 6\mathbf{u}^2\widetilde{\mathbf{F}}^2 + 3\rho\mathbf{u}^4,$$
$$\widetilde{\mathbf{F}}^5 \overset{\vee}{=} \mathbf{F}^5 + 5\mathbf{u}\widetilde{\mathbf{F}}^4 - 10\mathbf{u}^2\widetilde{\mathbf{F}}^3 + 10\mathbf{u}^3\widetilde{\mathbf{F}}^2 - 4\rho\mathbf{u}^5$$

to solve for the closing conserved moment.

Mapping from primitive to conserved variables

To express conserved moments in terms of primitive moments we observe that

$$\mathbf{v}^n \overset{\vee}{=} (\mathbf{u}+\mathbf{c})^n \overset{\vee}{=} \sum_{j=0}^{n} \binom{n}{j} \mathbf{u}^j \mathbf{c}^{n-j}.$$

Multiplying by $\mathcal{C}$ and integrating over velocity,

$$\widetilde{\mathbf{C}}^0 = \mathbf{C}^0,$$
$$\widetilde{\mathbf{C}}^1 = \mathbf{C}^1 + \mathbf{u}\mathbf{C}^0,$$
$$\widetilde{\mathbf{C}}^2 = \mathbf{C}^2 + 2\mathbf{u}\mathbf{C}^1 + \mathbf{u}^2\mathbf{C}^0,$$
$$\widetilde{\mathbf{C}}^3 \overset{\vee}{=} \mathbf{C}^3 + 3\mathbf{u}\mathbf{C}^2 + 3\mathbf{u}^2\mathbf{C}^1 + \mathbf{u}^3\mathbf{C}^0,$$
$$\widetilde{\mathbf{C}}^4 \overset{\vee}{=} \mathbf{C}^4 + 4\mathbf{u}\mathbf{C}^3 + 6\mathbf{u}^2\mathbf{C}^2 + 4\mathbf{u}^3\mathbf{C}^1 + \mathbf{u}^4\mathbf{C}^0,$$

where in the absence of production $\mathbf{C}^0 = 0$ and in the absence of interspecies friction $\mathbf{C}^1 = 0$.

Multiplying by f and integrating over velocity,

$$\widetilde{\mathbf{F}}^0 = \rho,$$
$$\widetilde{\mathbf{F}}^1 = \rho\mathbf{u},$$
$$\widetilde{\mathbf{F}}^2 = \mathbf{F}^2 + \rho\mathbf{u}^2,$$
$$\widetilde{\mathbf{F}}^3 \overset{\vee}{=} \mathbf{F}^3 + 3\mathbf{u}\mathbf{F}^2 + \rho\mathbf{u}^3,$$
$$\widetilde{\mathbf{F}}^4 \overset{\vee}{=} \mathbf{F}^4 + 4\mathbf{u}\mathbf{F}^3 + 6\mathbf{u}^2\mathbf{F}^2 + \rho\mathbf{u}^4,$$
$$\widetilde{\mathbf{F}}^5 \overset{\vee}{=} \mathbf{F}^5 + 5\mathbf{u}\mathbf{F}^4 + 10\mathbf{u}^2\mathbf{F}^3 + 10\mathbf{u}^3\mathbf{F}^2 + \rho\mathbf{u}^5,$$

where we have used that $\mathbf{F}^1 = 0$.

Collisional closures

Conventional names for primitive moments:

$$\mathbb{P} := \mathbf{F}^2, \qquad \mathbb{Q} := \mathbf{F}^3, \qquad \mathbb{R} := \mathbf{F}^4, \qquad \mathbb{S} := \mathbf{F}^5,$$
$$\delta_t\mathbb{P} := \mathbf{C}^2, \qquad \delta_t\mathbb{Q} := \mathbf{C}^3, \qquad \delta_t\mathbb{R} := \mathbf{C}^4.$$

Collisional moments for BGK collision operator:

$$\delta_t\mathbb{P} = -\frac{\mathbb{P}^\circ}{\tau},$$
$$\delta_t\mathbb{Q} = -\frac{\mathbb{Q}}{\tau_3},$$
$$\delta_t\mathbb{R} \overset{\vee}{=} \frac{3\mathbb{P}\mathbb{P}/\rho - \mathbb{R}}{\tau_4},$$

where $\mathbb{P}^\circ := \mathbb{P} - p\mathbb{I}$ is deviatoric pressure and for BGK $\tau = \tau_3 = \tau_4$.

Model coarsening:

- dial $\tau_4 \searrow 0$ to smoothly transition from 35-moment to 20-moment model.
- dial $\tau_3 \searrow 0$ to smoothly transition from 20-moment to 10-moment model.
- dial $\tau \searrow 0$ to smoothly transition to the 5-moment model.

and where when computing

$$\mathbf{C}^n = \frac{\int_{\mathbf{c}} \mathbf{c}^n (f_\theta - f)}{\widetilde{\tau}}$$

we have used that

$$\int_{\mathbf{c}} f_\theta = \rho,$$
$$\int_{\mathbf{c}} \mathbf{c} f_\theta = 0,$$
$$\int_{\mathbf{c}} \mathbf{c}\mathbf{c} f_\theta = \mathbb{P}$$
$$\int_{\mathbf{c}} \mathbf{c}\mathbf{c}\mathbf{c} f_\theta = 0, \text{ and}$$
$$\int_{\mathbf{c}} \mathbf{c}\mathbf{c}\mathbf{c}\mathbf{c} f_\theta \overset{\vee}{=} 3\mathbb{P}\mathbb{P}/\rho.$$

20-moment flux closure

20-moment Maxwellian-based closure [Grad49]

$$\mathbb{R} \overset{\vee}{=} 3(\mathbb{PP} - \mathbb{P}^{\circ}\mathbb{P}^{\circ})/\rho.$$

20-moment Gaussian-based closure [GrothGRB03]

$$\boxed{\mathbb{R} \overset{\vee}{=} 3\mathbb{PP}/\rho}.$$

Comparison of closures:

- The *Maxwellian-based* closure assumes that the velocity distribution is a *Maxwellian* times a polynomial.
- The *Gaussian-based* closure assumes that the velocity distribution is a *Gaussian* times a polynomial.
- Gaussian-based closure is a consistent generalization of the 10-moment model.
- Gaussian-based closure is hyperbolic if heat flux is small enough.
- Maxwellian-based closure is hyperbolic if heat flux and deviatoric stress are small enough.
- BGK would relax $\mathbb{R}$ to the Gaussian-based closure for $\mathbb{R}$.

Assumed distributions

- *Entropy-maximizing closure*:

  $$f(\mathbf{c}) = \exp(\mathbf{a} \cdot \mathbf{m}),$$

  where $\mathbf{m} = (1, \mathbf{cc}, \mathbf{ccc})$ is the tuple of evolved moments and $\mathbf{a}$ is a tuple of coefficients.
- *Maxwellian-based closure*

  $$f = W_M(1 + \mathbf{c}' \cdot \mathbf{m}),$$

  where

  $$W_M := \exp(\mathbf{c}_0 \cdot \mathbf{m}_0),$$

  $$\mathbf{m}_0 = (1, |\mathbf{c}|^2),$$

  and $\mathbf{c}' \cdot \mathbf{m}$ is a polynomial orthogonal to 1 and $|\mathbf{c}|^2$ in the weight W_M.
- *Gaussian-based closure*

  $$f = W_G(1 + \mathbf{c}' \cdot \mathbf{m}),$$

  where

  $$W_G := \exp(\mathbf{c}_0 \cdot \mathbf{m}_0),$$

  $$\mathbf{m}_0 = (1, \mathbf{cc}),$$

  and $\mathbf{c}' \cdot \mathbf{m}$ is a polynomial orthogonal to 1 and $\mathbf{cc}$ in the weight W_G.

35-moment flux closure (aside)

35-moment Gaussian-based closure [GrothGRB94]

$$\boxed{\mathbb{S} \overset{\vee}{=} 10\Theta\mathbb{Q}},$$

where $\Theta := \mathbb{P}/\rho$.

Remarks:

- Thoroughly studied in [GrothGRB94] and [Brown96].
- Large hyperbolicity region containing a Gaussian.
- Simple eigenstructure.

Assumed distributions

- *Entropy-maximizing closure*:

  $$f(\mathbf{c}) = \exp(\mathbf{a} \cdot \mathbf{m}),$$

  where $\mathbf{m} = (1, \mathbf{cc}, \mathbf{ccc}, \mathbf{cccc})$ is the tuple of evolved moments and $\mathbf{a}$ is a tuple of coefficients.

- *Maxwellian-based closure*

  $$f = W_M(1 + \mathbf{c}' \cdot \mathbf{m}),$$

  where

  $$W_M := \exp(\mathbf{c}_0 \cdot \mathbf{m}_0),$$

  $$\mathbf{m}_0 = (1, |\mathbf{c}|^2),$$

  and $\mathbf{c}' \cdot \mathbf{m}$ is a polynomial orthogonal to 1 and $|\mathbf{c}|^2$ in the weight W_M.

- *Gaussian-based closure*

  $$f = W_G(1 + \mathbf{c}' \cdot \mathbf{m}),$$

  where

  $$W_G := \exp(\mathbf{c}_0 \cdot \mathbf{m}_0),$$

  $$\mathbf{m}_0 = (1, \mathbf{cc}),$$

  and $\mathbf{c}' \cdot \mathbf{m}$ is a polynomial orthogonal to 1 and $\mathbf{cc}$ in the weight W_G.

Primitive moment evolution equations (aside)

Take primitive moments of the kinetic equation.

Relations for primitive moments:

$$
\begin{aligned}
\mathbf{c}(t,\mathbf{x},\mathbf{v}) &:= \mathbf{v} - \mathbf{u}(t,\mathbf{x}) \\
\int_{\mathbf{v}} &= \int_{\mathbf{c}} \\
\chi(t,\mathbf{x},\mathbf{v}) &= \chi(\mathbf{c}) = \mathbf{c}^n \\
\nabla_{\mathbf{v}}\chi &= \nabla_{\mathbf{c}}\chi \\
\mathrm{d}_t^{\mathbf{v}} &:= \partial_t + \mathbf{v}\cdot\nabla_{\mathbf{x}} \\
\rho\langle\alpha\rangle &:= \int_{\mathbf{v}}\alpha \\
\bar{D}_t(\alpha) &:= \partial_t\alpha + \nabla_{\mathbf{x}}\cdot(\mathbf{v}\alpha) + \nabla_{\mathbf{v}}\cdot(\mathbf{a}\alpha) \\
D_t &:= \partial_t + \mathbf{v}\cdot\nabla_{\mathbf{x}} + \mathbf{a}\cdot\nabla_{\mathbf{v}} = \bar{D}_t \\
\bar{D}_t(\alpha\beta) &= (\bar{D}_t\alpha)\beta + \alpha D_t\beta
\end{aligned}
$$

Multiply the kinetic equation

$$\bar{D}_t f = C$$

by χ to get

$$\boxed{\bar{D}_t(\chi f) = f D_t\chi + \chi\mathcal{C}.} \tag{2}$$

But observe that for $\chi(\mathbf{c})$:

$$
\begin{aligned}
D_t &= \mathrm{d}_t^{\mathbf{v}} + \mathbf{a}\cdot\nabla_{\mathbf{v}}\cdot, \\
\mathrm{d}_t^{\mathbf{v}}\chi &= (\mathrm{d}_t^{\mathbf{v}}\mathbf{c})\cdot\nabla_{\mathbf{c}}\chi \\
&= -(\mathrm{d}_t^{\mathbf{v}}\mathbf{u})\cdot\nabla_{\mathbf{c}}\chi, \\
\mathrm{d}_t^{\mathbf{v}} &= \mathrm{d}_t^{\mathbf{u}} + \mathbf{c}\cdot\nabla_{\mathbf{x}};
\end{aligned}
$$

putting it together,

$$D_t\chi = \left(\mathbf{a} - \mathrm{d}_t^{\mathbf{u}}\mathbf{u} - \mathbf{c}\cdot\nabla_{\mathbf{x}}\mathbf{u}\right)\cdot\nabla_{\mathbf{c}}\chi \tag{3}$$

But solving momentum evolution

$$\rho\mathrm{d}_t^{\mathbf{u}}\mathbf{u} + \nabla\cdot\mathbf{P}^2 = \rho\langle\mathbf{a}\rangle + \mathbf{C}^1$$

for $\mathrm{d}_t^{\mathbf{u}}\mathbf{u}$, substituting in (3), and defining

$$\mathbf{a}' := \mathbf{a} - \langle\mathbf{a}\rangle = \frac{q}{m}\mathbf{c}\times\mathbf{B}$$

gives

$$\boxed{
\begin{aligned}
D_t\chi = &\left(\mathbf{a}' - \mathbf{c}\cdot\nabla_{\mathbf{x}}\mathbf{u}\right)\cdot\nabla_{\mathbf{c}}\chi \\
&+ \frac{\nabla\cdot\mathbf{P}^2 - \mathbf{C}^1}{\rho}\cdot\nabla_{\mathbf{c}}\chi.
\end{aligned}
} \tag{4}$$

Substituting (4) into the kinetic equation (2) and integrating over velocity space yields:

$$\partial_t(\rho\langle\chi\rangle) + \nabla\cdot(\rho\mathbf{u}\langle\chi\rangle) + \nabla\cdot(\rho\langle\mathbf{c}\chi\rangle) = (\nabla\cdot\mathbf{P}^2 - \mathbf{C}^1)\cdot\langle\nabla_{\mathbf{c}}\chi\rangle + \rho\left\langle\left(\mathbf{a}' - \mathbf{c}\cdot\nabla\mathbf{u}\right)\cdot\nabla_{\mathbf{c}}\chi\right\rangle + \int_{\mathbf{v}}\chi\mathcal{C}. \tag{5}$$

Now impose that $\chi(\mathbf{c}) = \mathbf{c}^n$. For a generic $\underline{\alpha}$, $\underline{\alpha}\cdot\nabla_{\mathbf{c}}\left(\mathbf{c}^n\right) = n\,\mathrm{Sym}\left(\underline{\alpha}\mathbf{c}^{n-1}\right)$. So

$$\rho\left\langle(\mathbf{a}' - \mathbf{c}\cdot\nabla\mathbf{u})\cdot\nabla_{\mathbf{c}}\mathbf{c}^n\right\rangle = n\rho\,\mathrm{Sym}\left\langle(\mathbf{a}' - \mathbf{c}\cdot\nabla\mathbf{u})\mathbf{c}^{n-1}\right\rangle = n\,\mathrm{Sym}\left(\tfrac{q}{m}\mathbf{P}^n\times\mathbf{B} - \mathbf{P}^n\cdot\nabla\mathbf{u}\right) \tag{6}$$

Substituting identity (6) into equation (5) gives an evolution equation for primitive moments:

$$\rho d_t\bar{\mathbf{P}}^n + n\,\mathrm{Sym}\left(\bar{\mathbf{P}}^{n-1}(\mathbf{C}^1 - \nabla\cdot\mathbf{P}^2) + \mathbf{P}^n\cdot\nabla\mathbf{u}\right) + \nabla\cdot\mathbf{P}^{n+1} = n\,\mathrm{Sym}\left(\tfrac{q}{m}\mathbf{P}^n\times\mathbf{B}\right) + \mathbf{C}^n, \tag{7}$$

where $\bar{\mathbf{P}}^n := \langle\mathbf{c}^n\rangle = \mathbf{P}^n/\rho$. and $d_t := \partial_t + \mathbf{u}\cdot\nabla$.

Primitive quasilinear form (aside)

Equation (7) can also be written:

$$\boxed{\rho d_t \mathbf{F}^n - n\bar{\mathbf{F}}^{n-1}\nabla\cdot\mathbf{F}^2 + n\mathbf{F}^n\cdot\nabla\mathbf{u} + \nabla\cdot\mathbf{F}^{n+1} \stackrel{\vee}{=} n\tfrac{q}{m}\mathbf{F}^n\times\mathbf{B} - n\bar{\mathbf{F}}^{n-1}\mathbf{C}^1 + \mathbf{C}^n},$$

which is an evolution equation for the generalized temperature $\bar{\mathbf{F}}^n$.

The **35-moment system in quasilinear form** is thus

$$\boxed{\begin{aligned}
d_t\rho + \rho\nabla\cdot\mathbf{u} &= \mathbf{C}^0 = 0,\\
\rho d_t\mathbf{u} + \nabla\cdot\mathbf{F}^2 &= \tfrac{q}{m}\rho(\mathbf{E}+\mathbf{u}\times\mathbf{B}) + \mathbf{C}^1,\\
\rho d_t\bar{\mathbf{F}}^2 + 2\mathbf{F}^2\cdot\nabla\mathbf{u} + \nabla\cdot\mathbf{F}^3 &\stackrel{\vee}{=} 2\tfrac{q}{m}\mathbf{F}^2\times\mathbf{B} + \mathbf{C}^2,\\
\rho d_t\bar{\mathbf{F}}^3 - 3\bar{\mathbf{F}}^2\nabla\cdot\mathbf{F}^2 + 3\mathbf{F}^3\cdot\nabla\mathbf{u} + \nabla\cdot\mathbf{F}^4 &\stackrel{\vee}{=} 3\tfrac{q}{m}\mathbf{F}^3\times\mathbf{B} - 3\bar{\mathbf{F}}^2\mathbf{C}^1 + \mathbf{C}^3,\\
\rho d_t\bar{\mathbf{F}}^4 - 4\bar{\mathbf{F}}^3\nabla\cdot\mathbf{F}^2 + 4\mathbf{F}^4\cdot\nabla\mathbf{u} + \nabla\cdot\mathbf{F}^5 &\stackrel{\vee}{=} 4\tfrac{q}{m}\mathbf{F}^4\times\mathbf{B} - 4\bar{\mathbf{F}}^3\mathbf{C}^1 + \mathbf{C}^4,
\end{aligned}}$$

which generalizes equations (4.15) through (4.19) in [GrothGRB03] and agrees if $\mathbf{C}^0 = 0$ (as implicitly assumed on the previous slide).

Outline

Magnetic Reconnection

- Magnetic field lines are convected with plasma except near reconnection point.
- Adjacent oppositely directed magnetic field lines field lines come together and cancel and reconnect.
- Oppositely directed jets form along outflow axis.

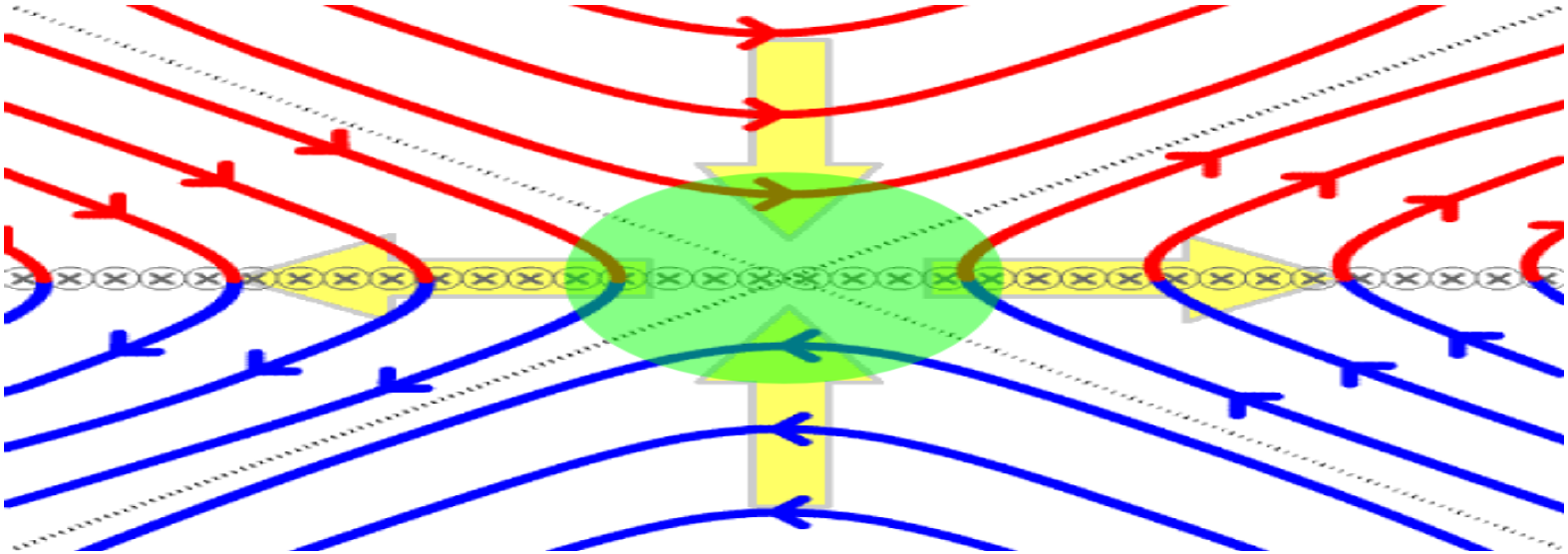

2D separator steady reconnection

Magnetic Reconnection

- Magnetic field lines are convected with plasma except near reconnection point.
- Adjacent oppositely directed magnetic field lines field lines come together and cancel and reconnect.
- Oppositely directed jets form along outflow axis.

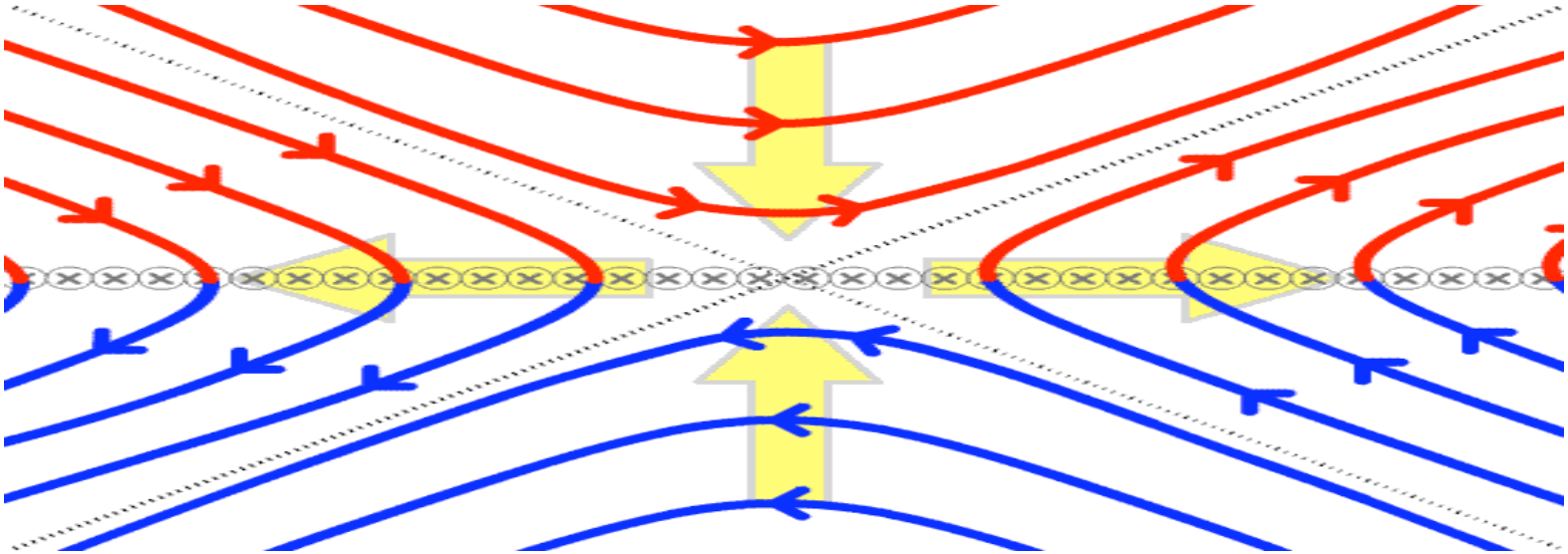

2D separator steady reconnection

Magnetic Reconnection

- Magnetic field lines are convected with plasma except near reconnection point.
- Adjacent oppositely directed magnetic field lines field lines come together and cancel and reconnect.
- Oppositely directed jets form along outflow axis.

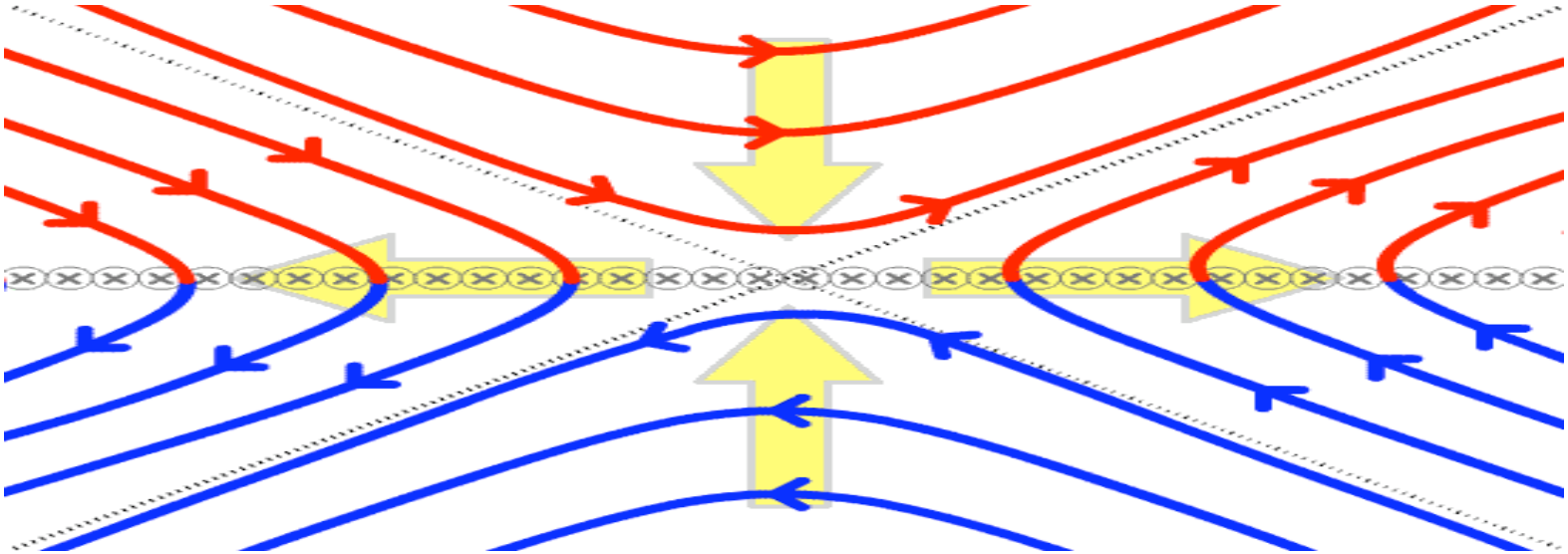

2D separator steady reconnection

Magnetic Reconnection

- Magnetic field lines are convected with plasma except near reconnection point.
- Adjacent oppositely directed magnetic field lines field lines come together and cancel and reconnect.
- Oppositely directed jets form along outflow axis.

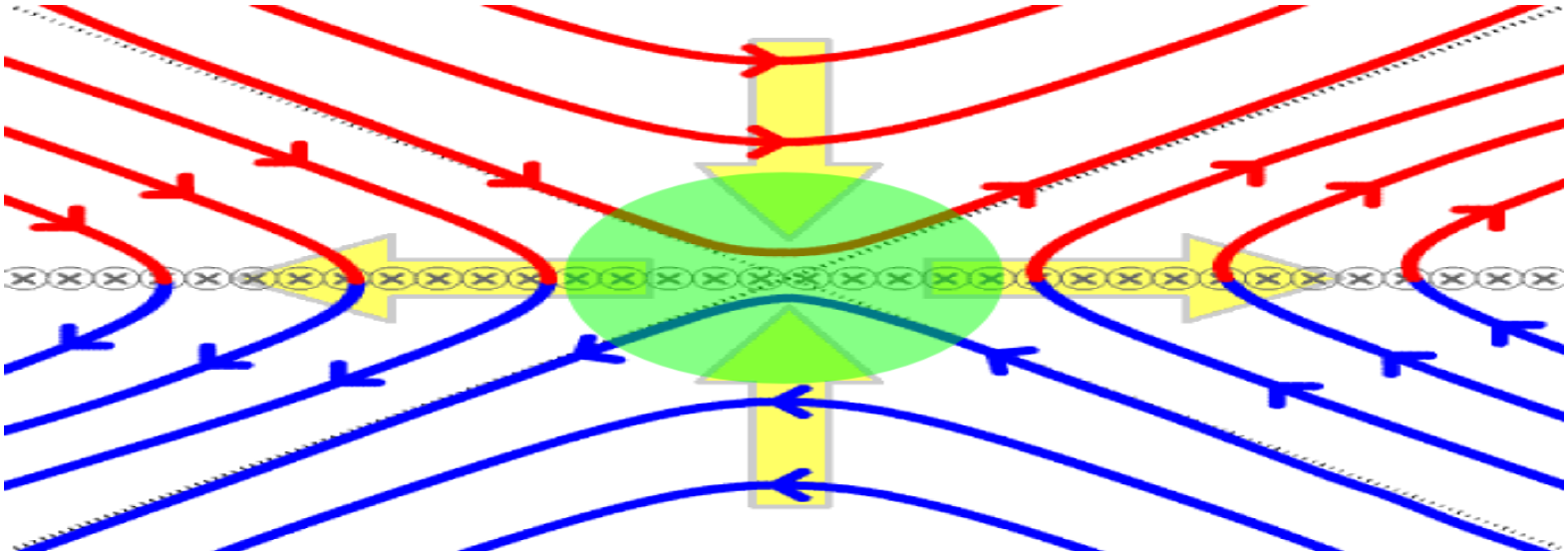

2D separator steady reconnection

Magnetic Reconnection

- Magnetic field lines are convected with plasma except near reconnection point.
- Adjacent oppositely directed magnetic field lines field lines come together and cancel and reconnect.
- Oppositely directed jets form along outflow axis.

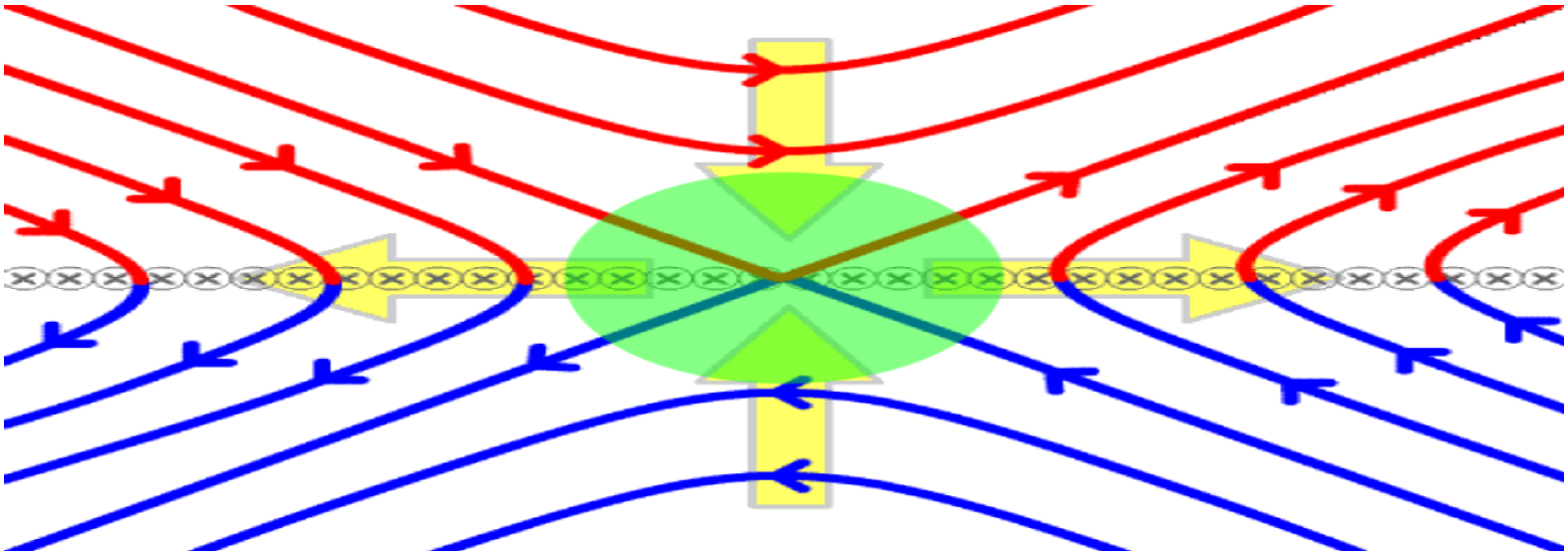

2D separator steady reconnection

Magnetic Reconnection

- Magnetic field lines are convected with plasma except near reconnection point.
- Adjacent oppositely directed magnetic field lines field lines come together and cancel and reconnect.
- Oppositely directed jets form along outflow axis.

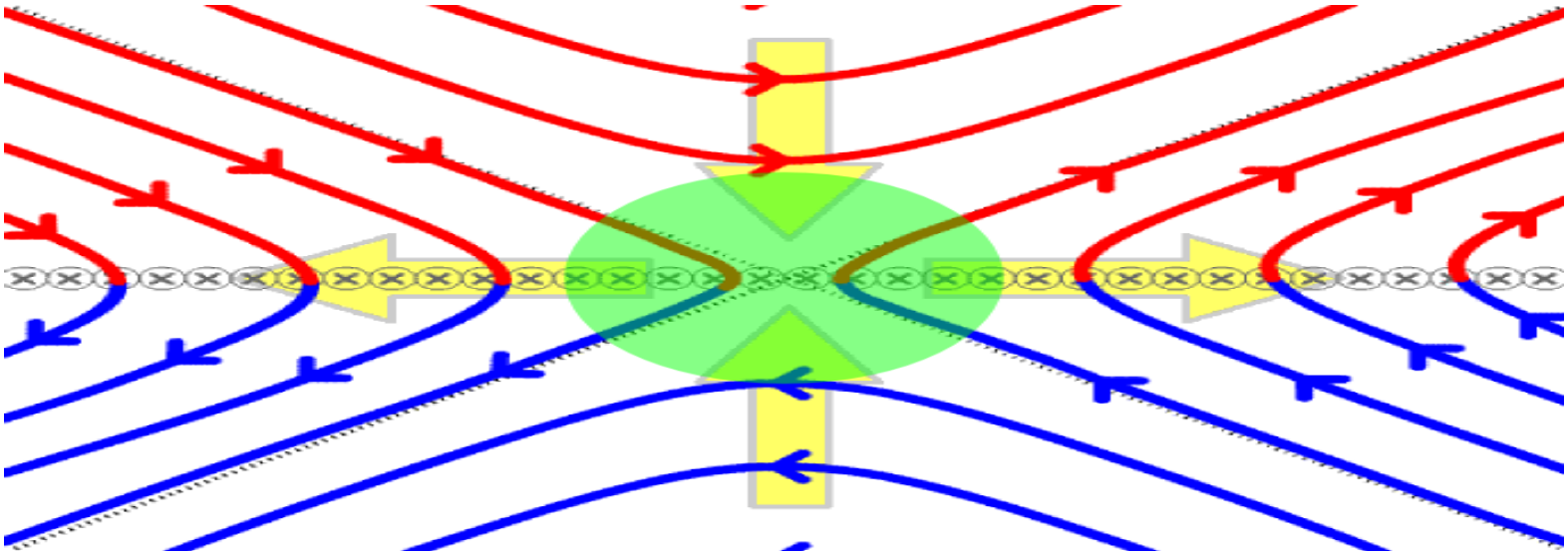

2D separator steady reconnection

Magnetic Reconnection

- Magnetic field lines are convected with plasma except near reconnection point.
- Adjacent oppositely directed magnetic field lines field lines come together and cancel and reconnect.
- Oppositely directed jets form along outflow axis.

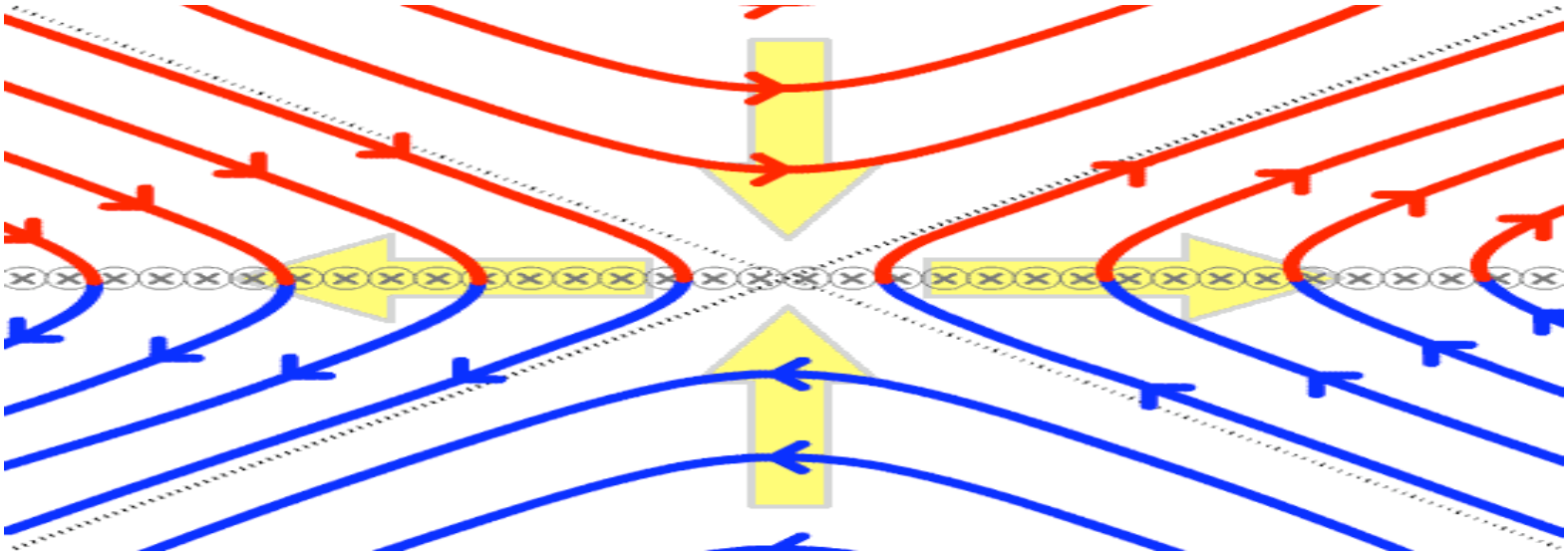

2D separator steady reconnection

Magnetic Reconnection

- Magnetic field lines are convected with plasma except near reconnection point.
- Adjacent oppositely directed magnetic field lines field lines come together and cancel and reconnect.
- Oppositely directed jets form along outflow axis.

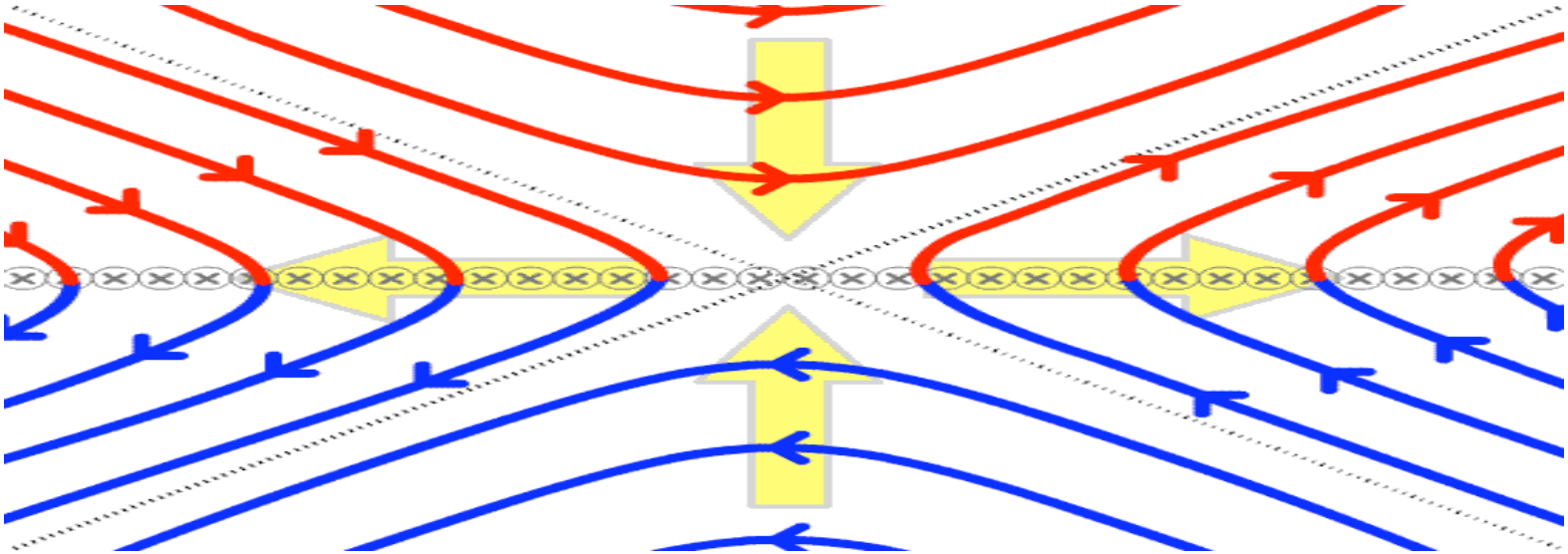

2D separator steady reconnection

Magnetic Reconnection

- Magnetic field lines are convected with plasma except near reconnection point.
- Adjacent oppositely directed magnetic field lines field lines come together and cancel and reconnect.
- Oppositely directed jets form along outflow axis.

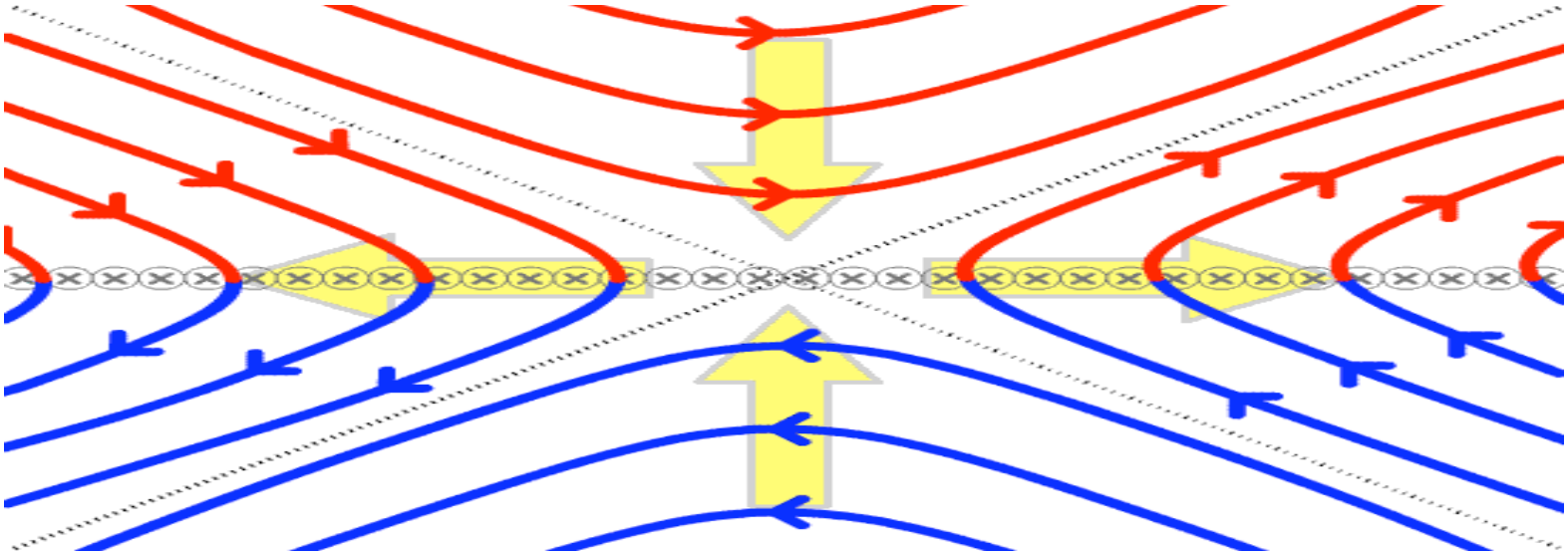

2D separator steady reconnection

Dynamic reconnection: GEM challenge problem [GEM01]

The GEM problem initiates reconnection by pinching adjacent oppositely directed field lines.

Two-fluid simulations suggest qualitative agreement with kinetic simulations:

- Vlasov-Darwin simulations: [SchmitzGrauer06]
- 5-moment two-fluid-Maxwell simulations: [HaLoSh06], [LoHaSh11].
- 10-moment two-fluid-Maxwell simulations: [Hakim06], [JoRo10], [Jo11].
- 20-moment two-fluid-Maxwell simulations: [see the following slides]

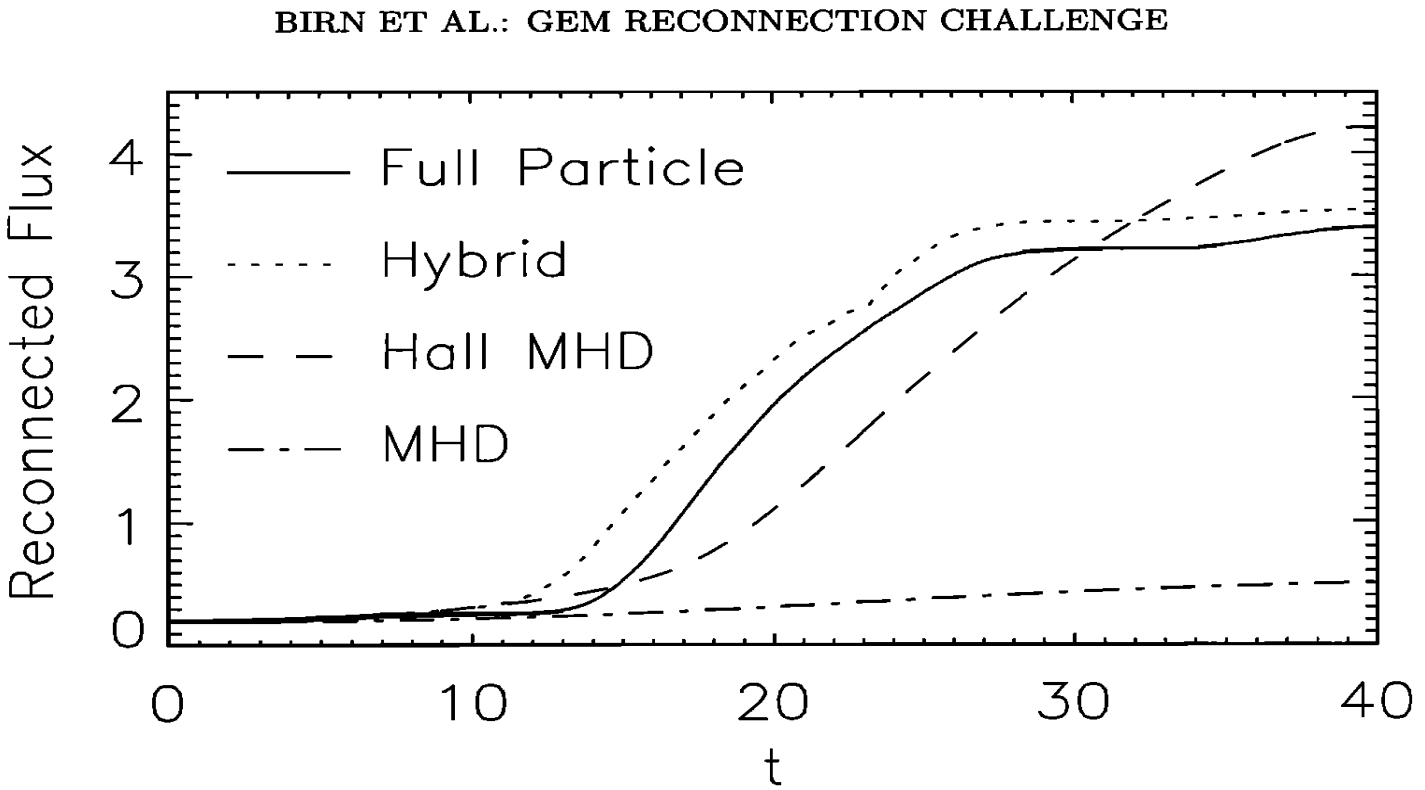

Figure 1. The reconnected magnetic flux versus time from a variety of simulation models: full particle, hybrid, Hall MHD, and MHD (for resistivity $\eta = 0.005$).

Simulation parameters

- Symmetry is enforced and system is solved on a quarter-domain for all simulations.
- All fluid simulations use a 32x64 computational mesh.
- 3rd-order Runge-Kutta discontinuous Galerkin
- time scale is ion gyroperiod.
- Alfvén speed is nondimensionalized to 1.
- so spatial scale is ion skin depth.
- light speed is 20.
- relaxation period is chosen to be $\tau_s = 50\sqrt{\det \Theta_s}/\rho_s$.
- simulations were run until they crashed on negative pressure (positivity limiting not yet implemented).

Reconnecting flux for 10-moment model

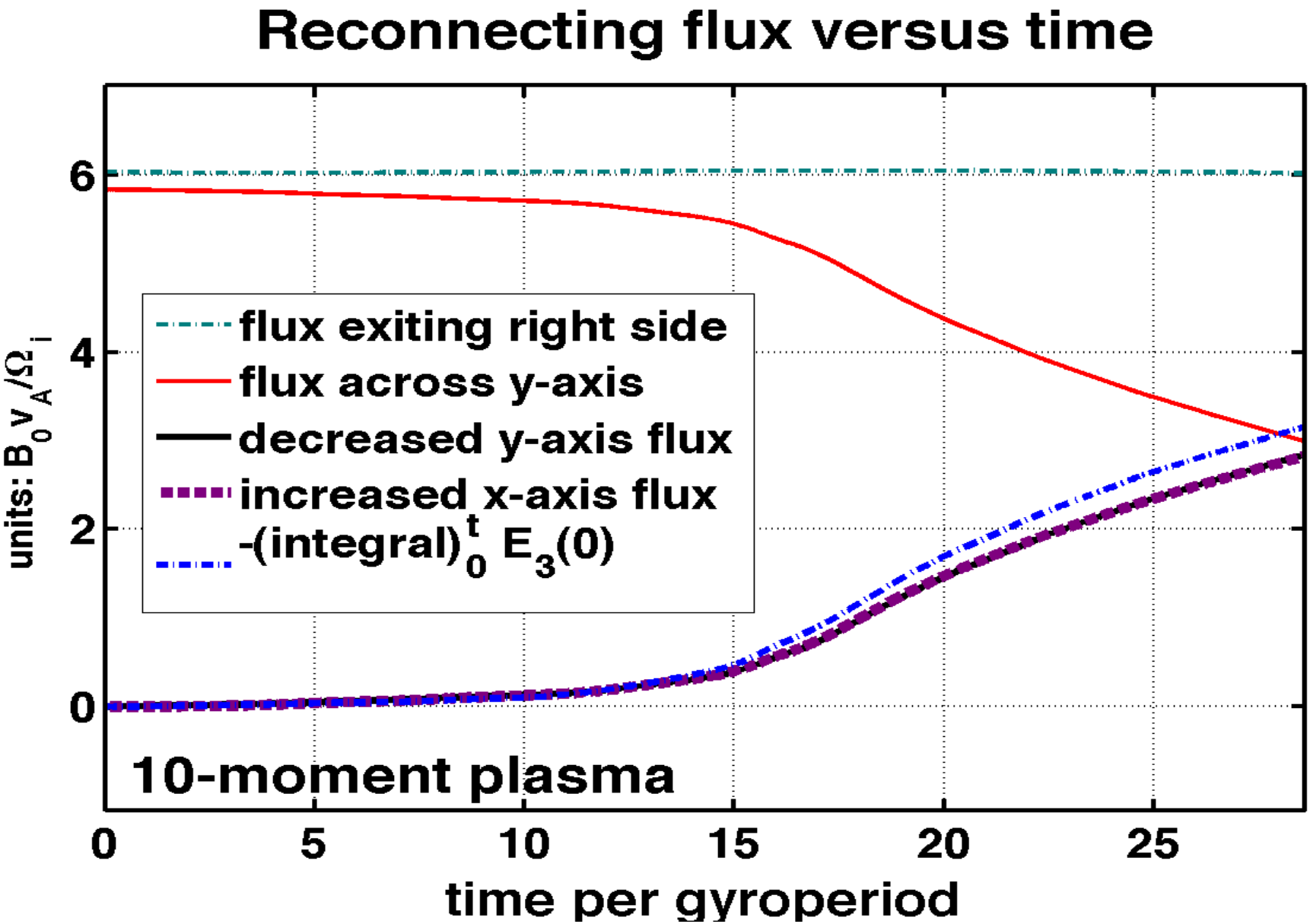

Reconnecting flux for 10-moment model (again)

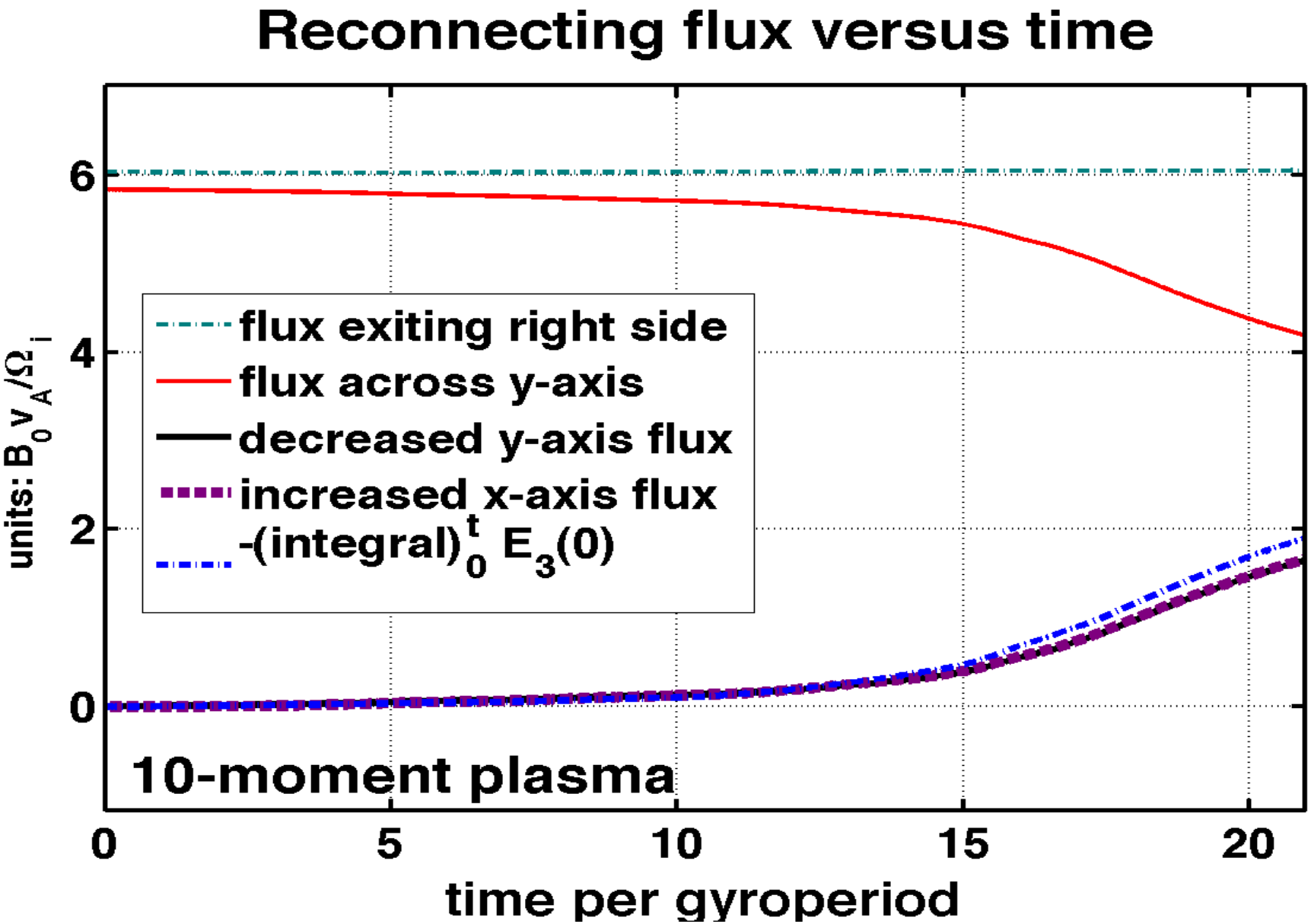

Reconnecting flux for 20-moment model

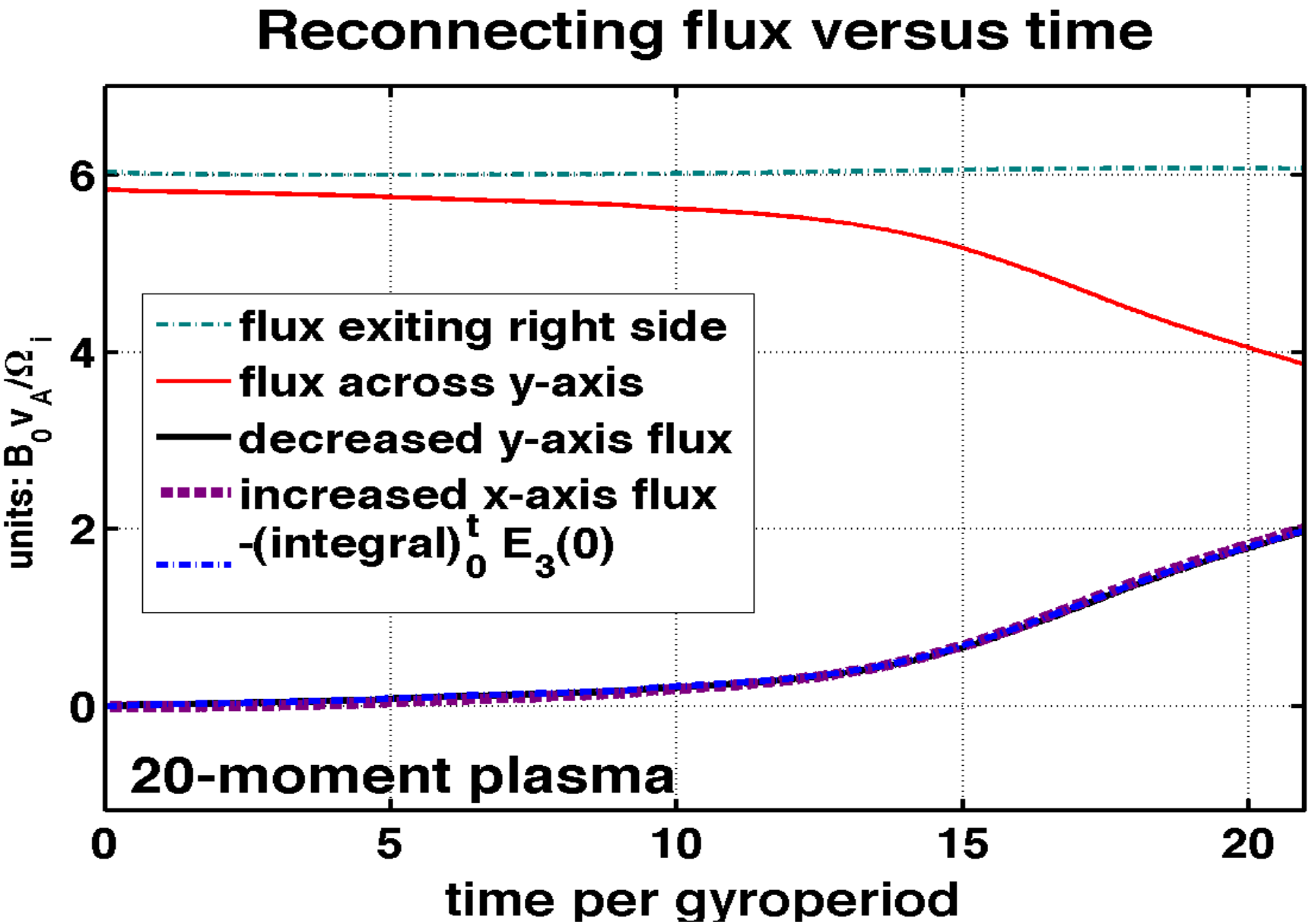

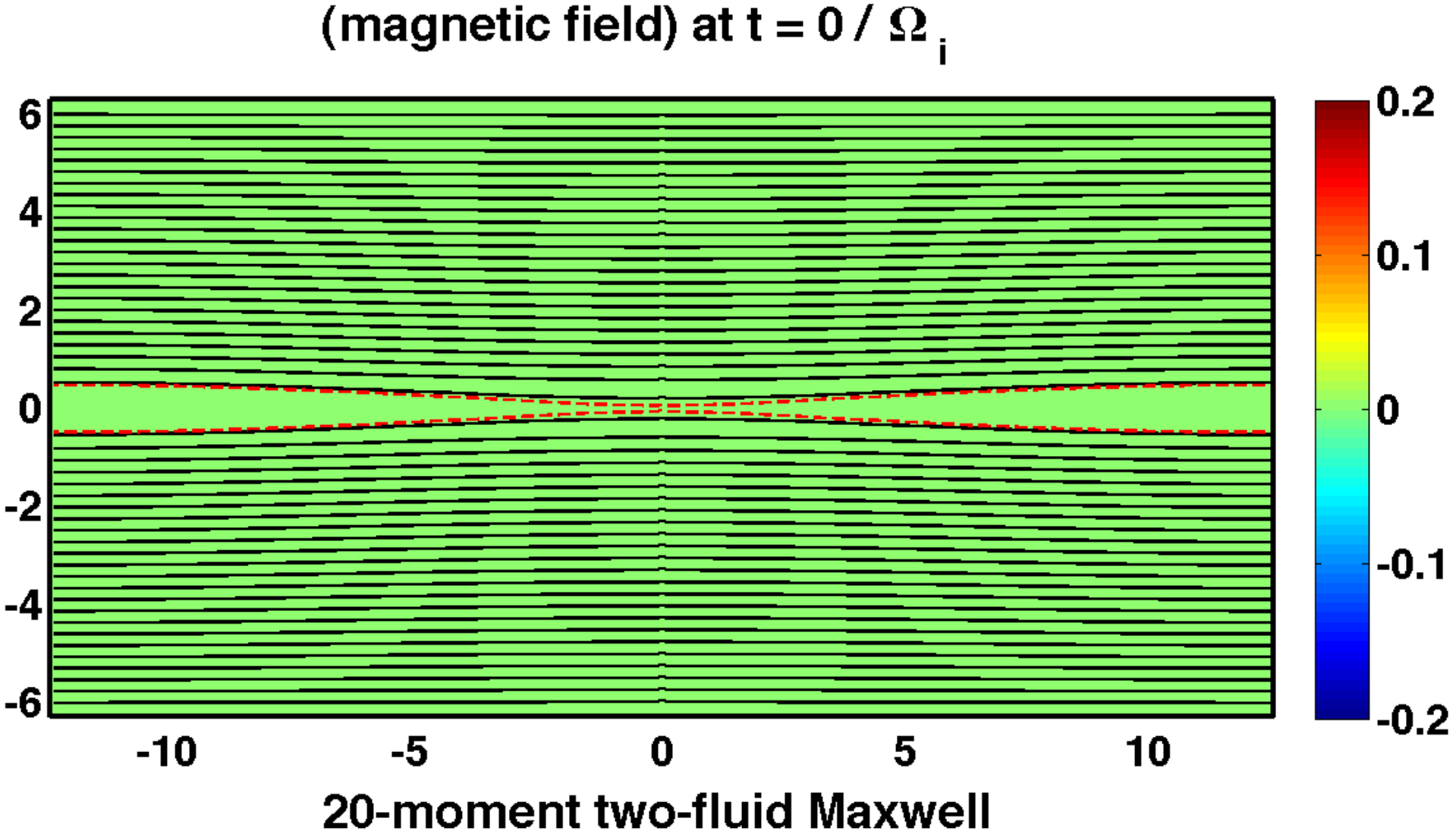
(magnetic field) at t = 0 / Ω i
6
4
2
0
-2
-4
-6
-10
-5
0
5
10
0.2
0.1
0
-0.1
-0.2
20-moment two-fluid Maxwell

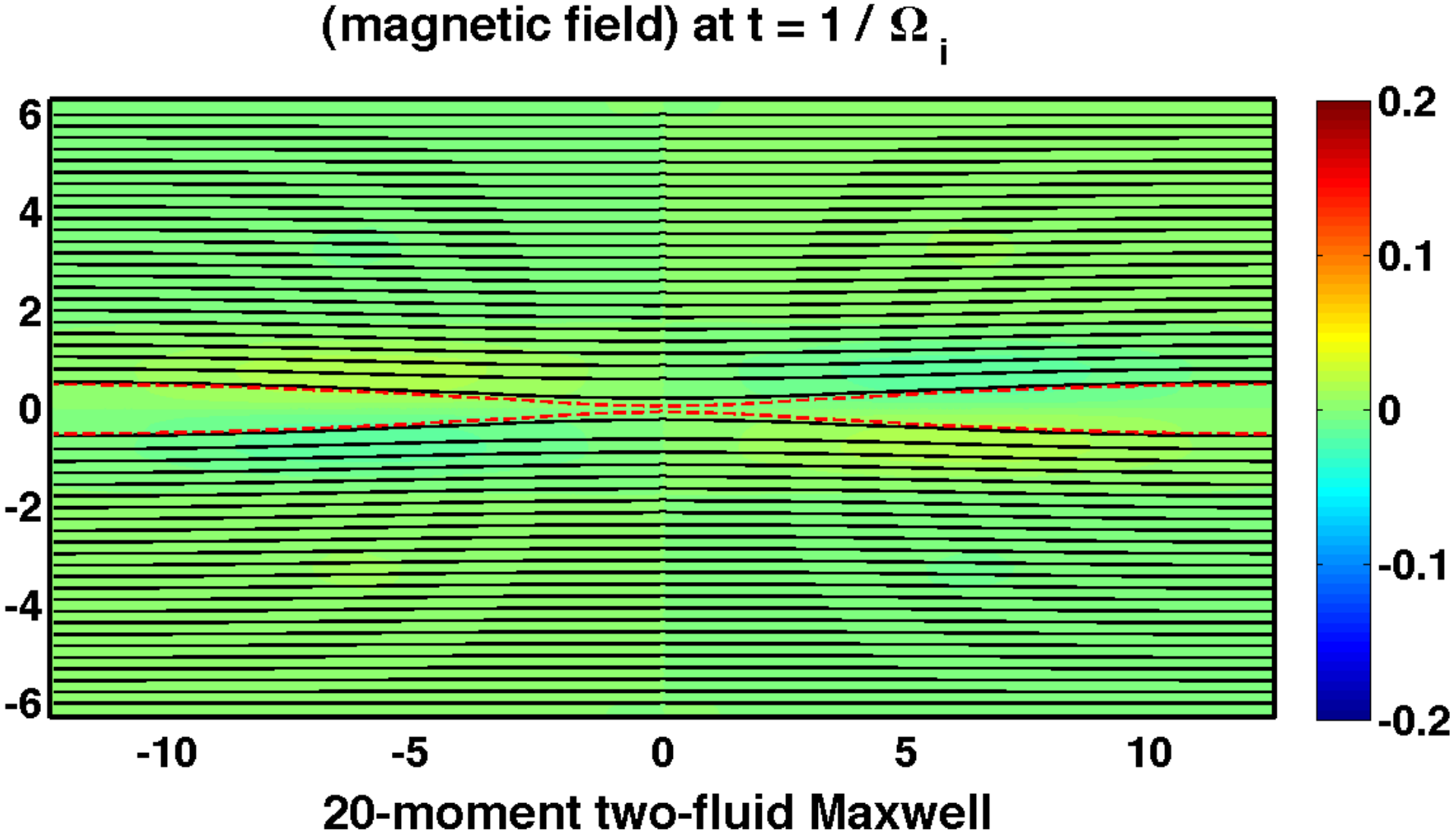
(magnetic field) at t = 1 / Ω i
6
4
2
0
-2
-4
-6
-10
-5
0
5
10
0.2
0.1
0
-0.1
-0.2
20-moment two-fluid Maxwell

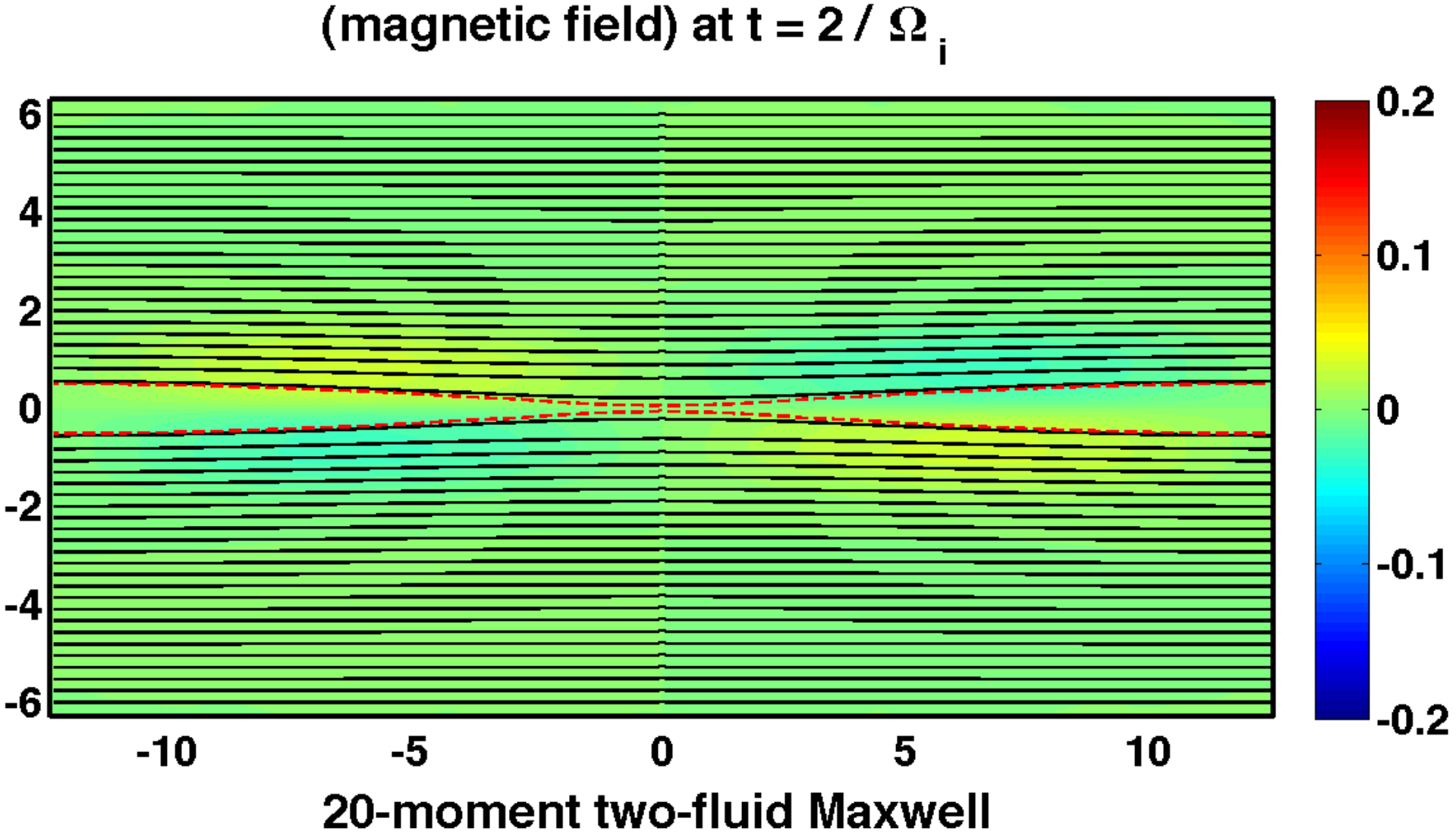
(magnetic field) at t = 2 / Ω i
6
4
2
0
-2
-4
-6
-10
-5
0
5
10
0.2
0.1
0
-0.1
-0.2
20-moment two-fluid Maxwell

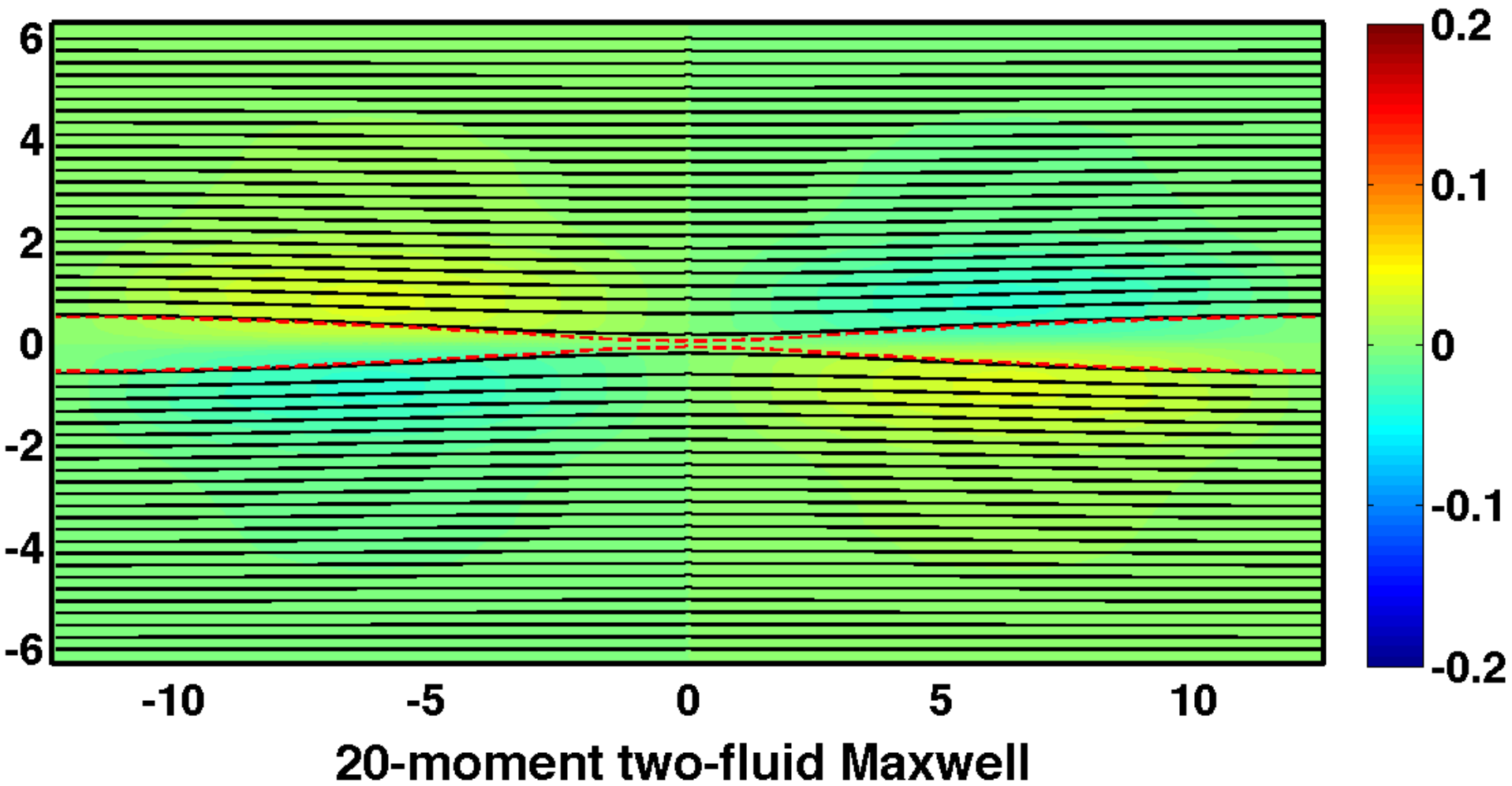
(magnetic field) at t = 3 / Ω i
6
4
2
0
-2
-4
-6
-10
-5
0
5
10
0.2
0.1
0
-0.1
-0.2
20-moment two-fluid Maxwell

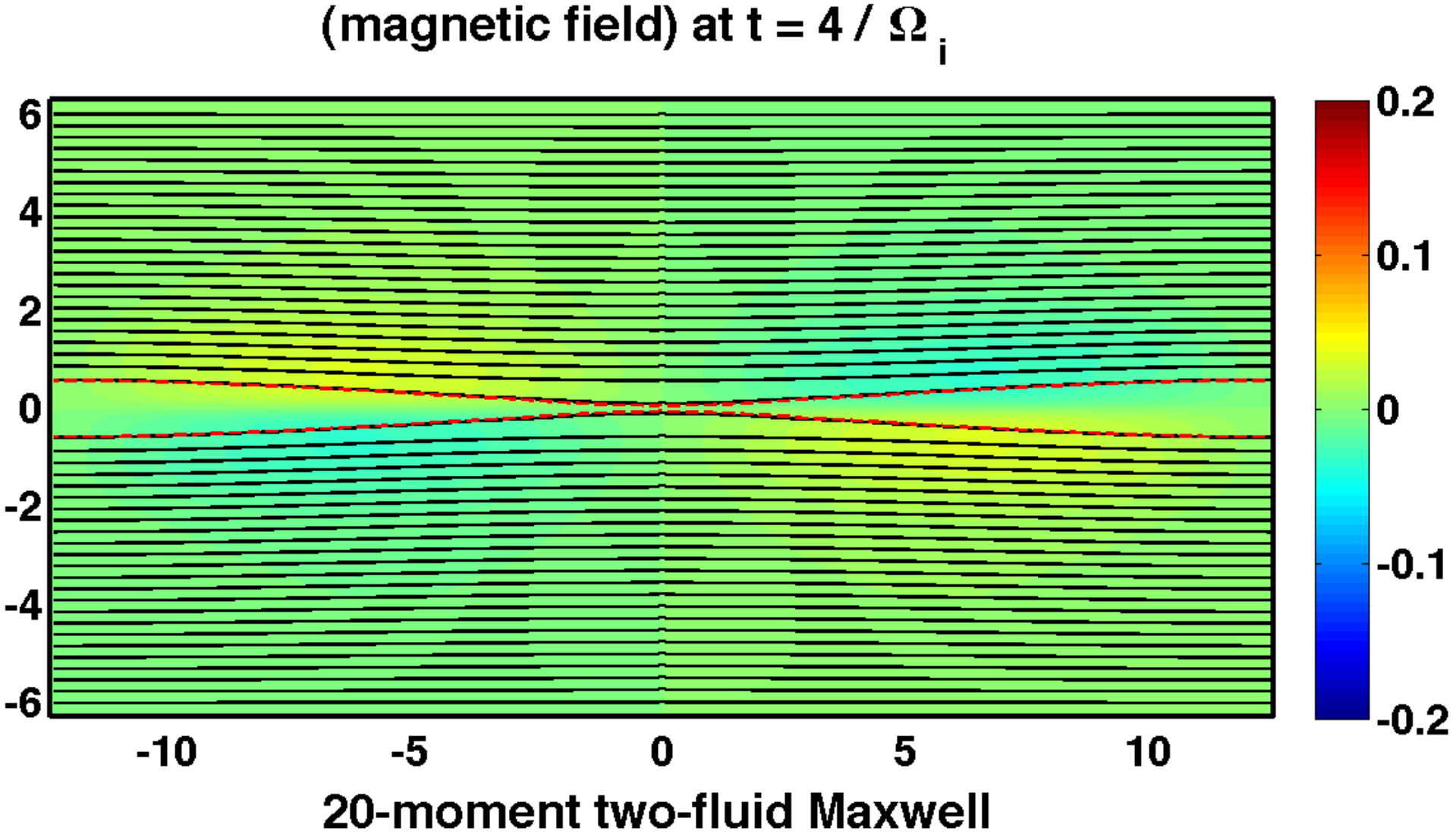
(magnetic field) at t = 4 / Ω i
6
4
2
0
-2
-4
-6
-10
-5
0
5
10
0.2
0.1
0
-0.1
-0.2
20-moment two-fluid Maxwell

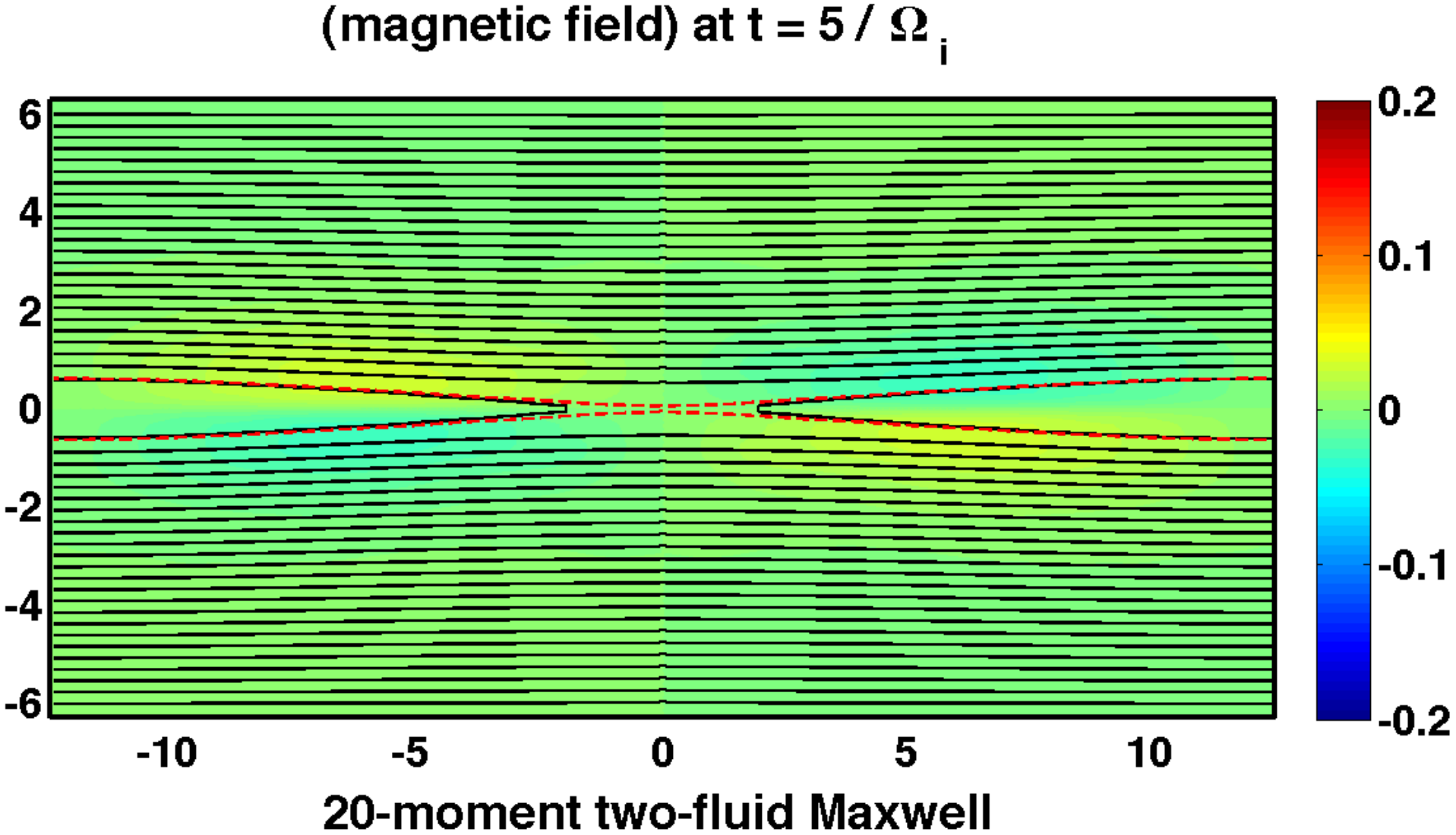
(magnetic field) at t = 5 / Ω i
6
4
2
0
-2
-4
-6
-10
-5
0
5
10
0.2
0.1
0
-0.1
-0.2
20-moment two-fluid Maxwell

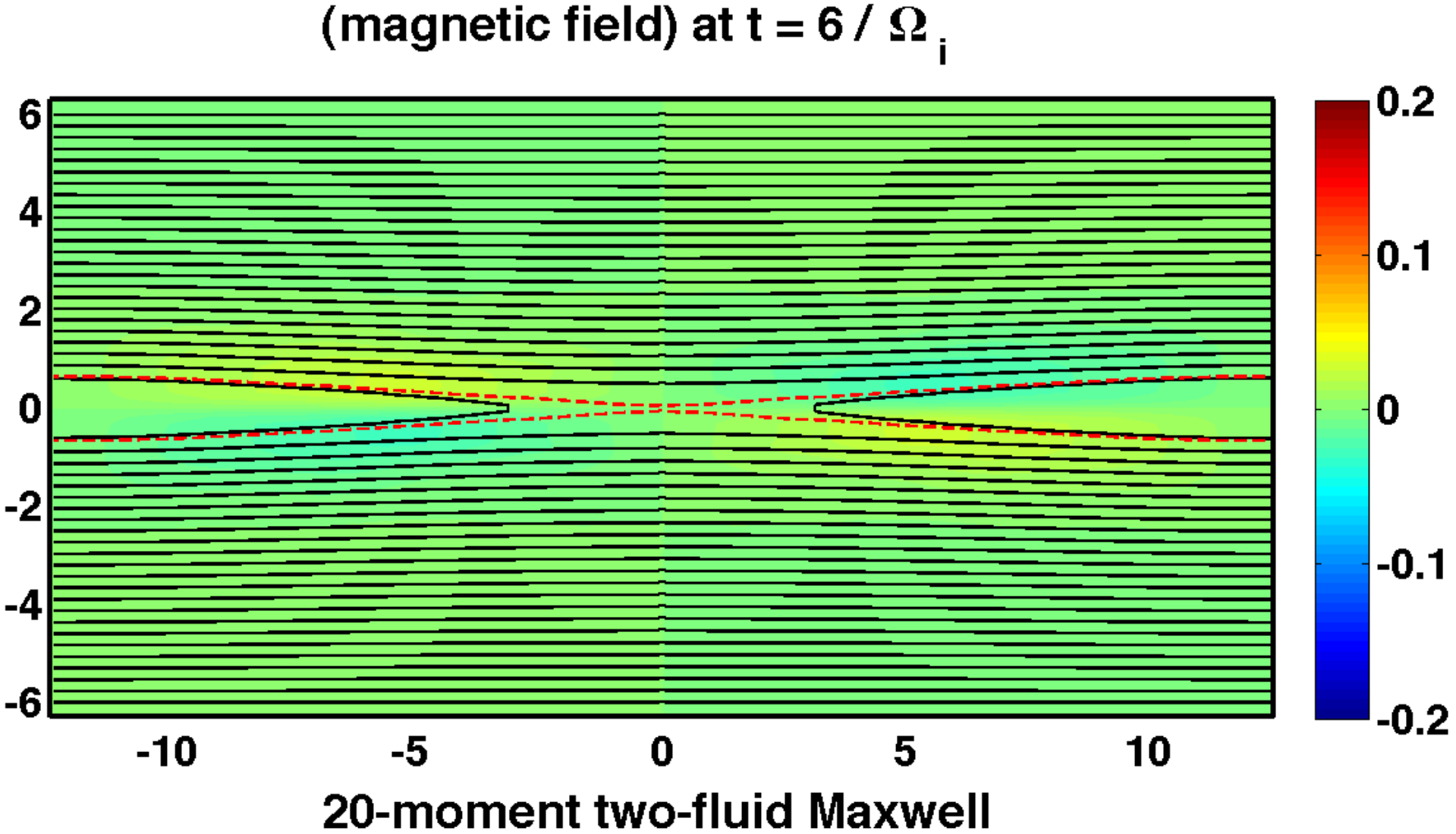
(magnetic field) at t = 6 / Ω i
6
4
2
0
-2
-4
-6
-10
-5
0
5
10
0.2
0.1
0
-0.1
-0.2
20-moment two-fluid Maxwell

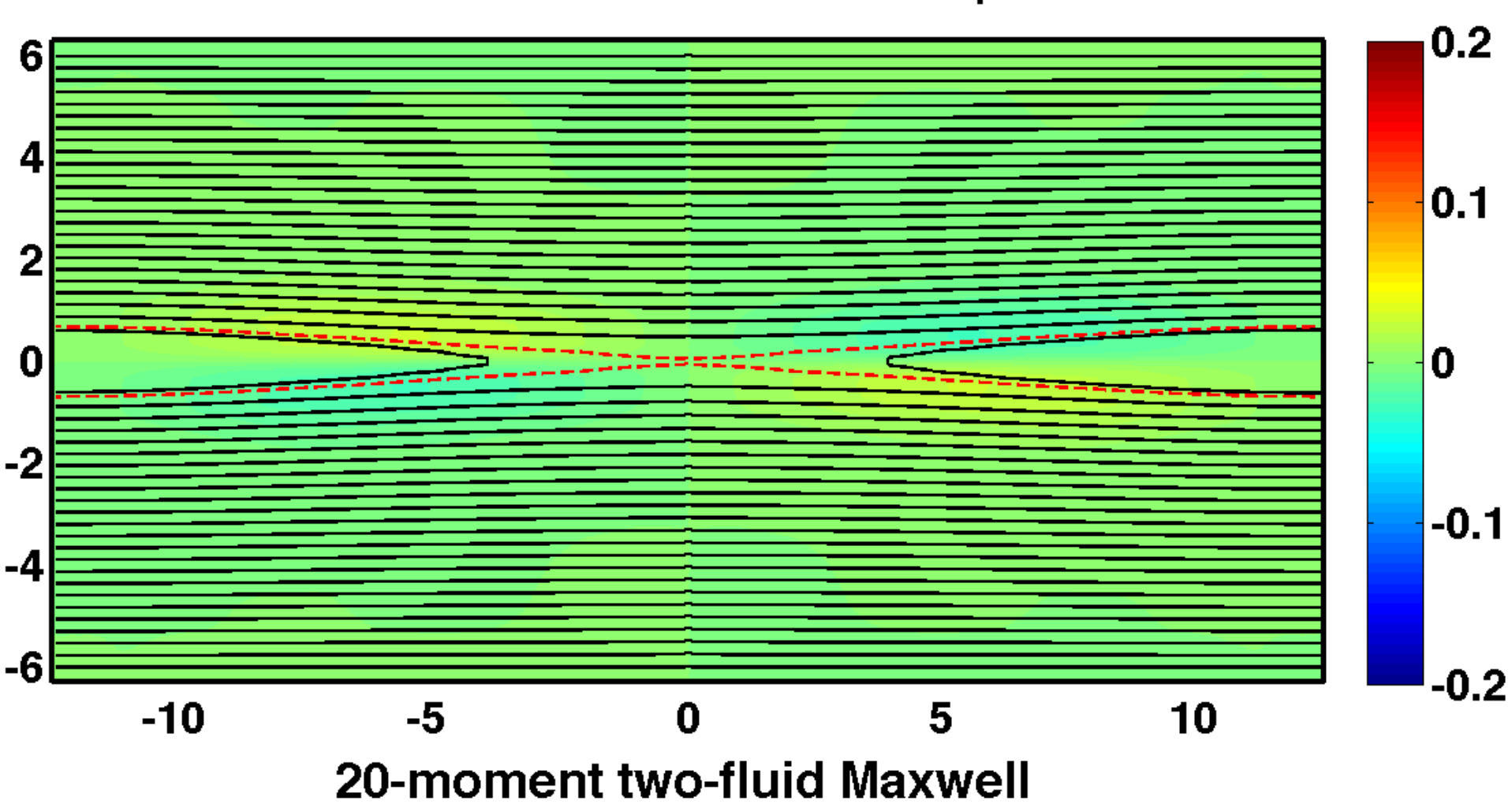
(magnetic field) at t = 7 / Ω i
6
4
2
0
-2
-4
-6
-10
-5
0
5
10
0.2
0.1
0
-0.1
-0.2
20-moment two-fluid Maxwell

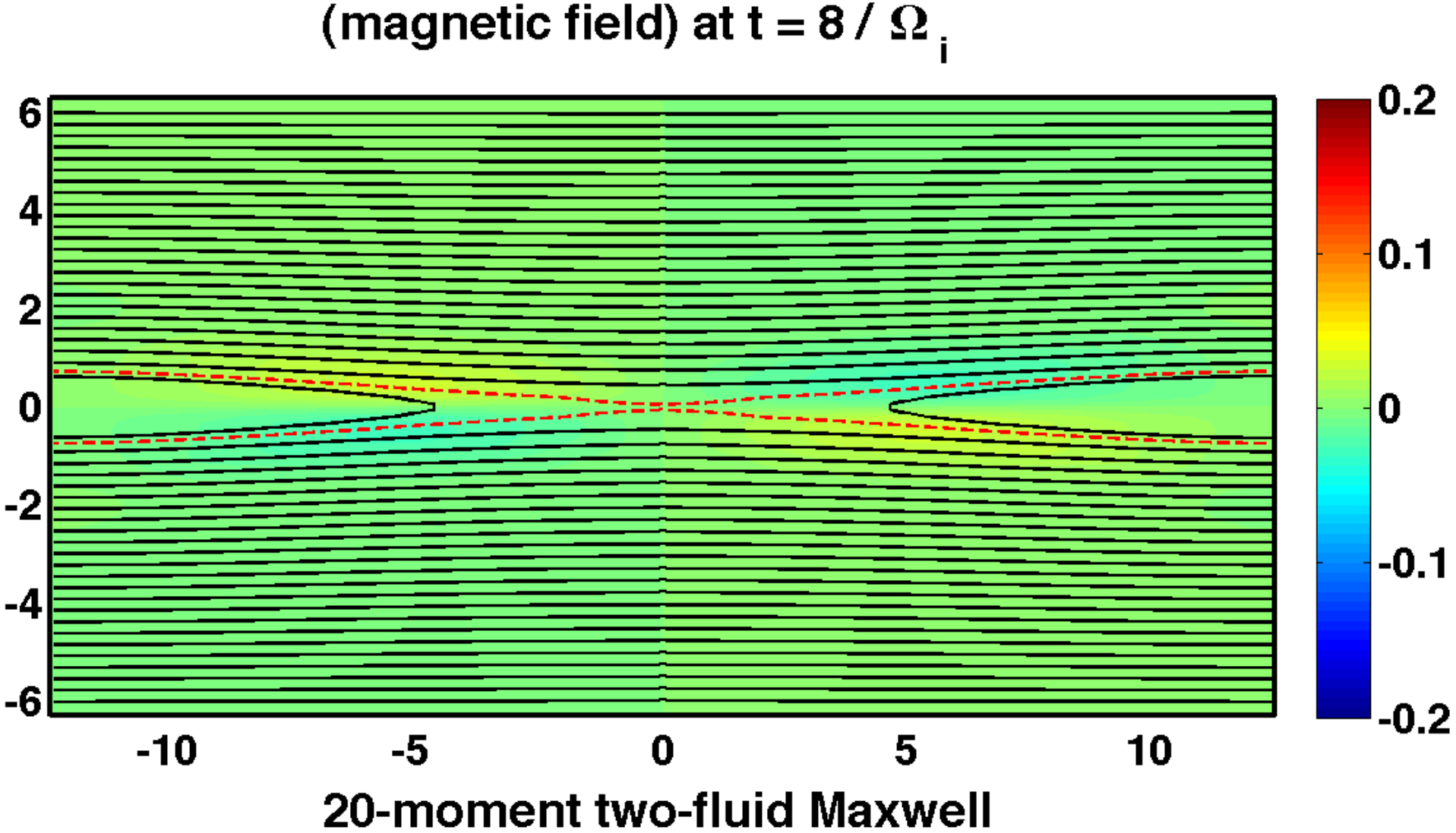
(magnetic field) at t = 8 / Ω i
6
4
2
0
-2
-4
-6
-10
-5
0
5
10
0.2
0.1
0
-0.1
-0.2
20-moment two-fluid Maxwell

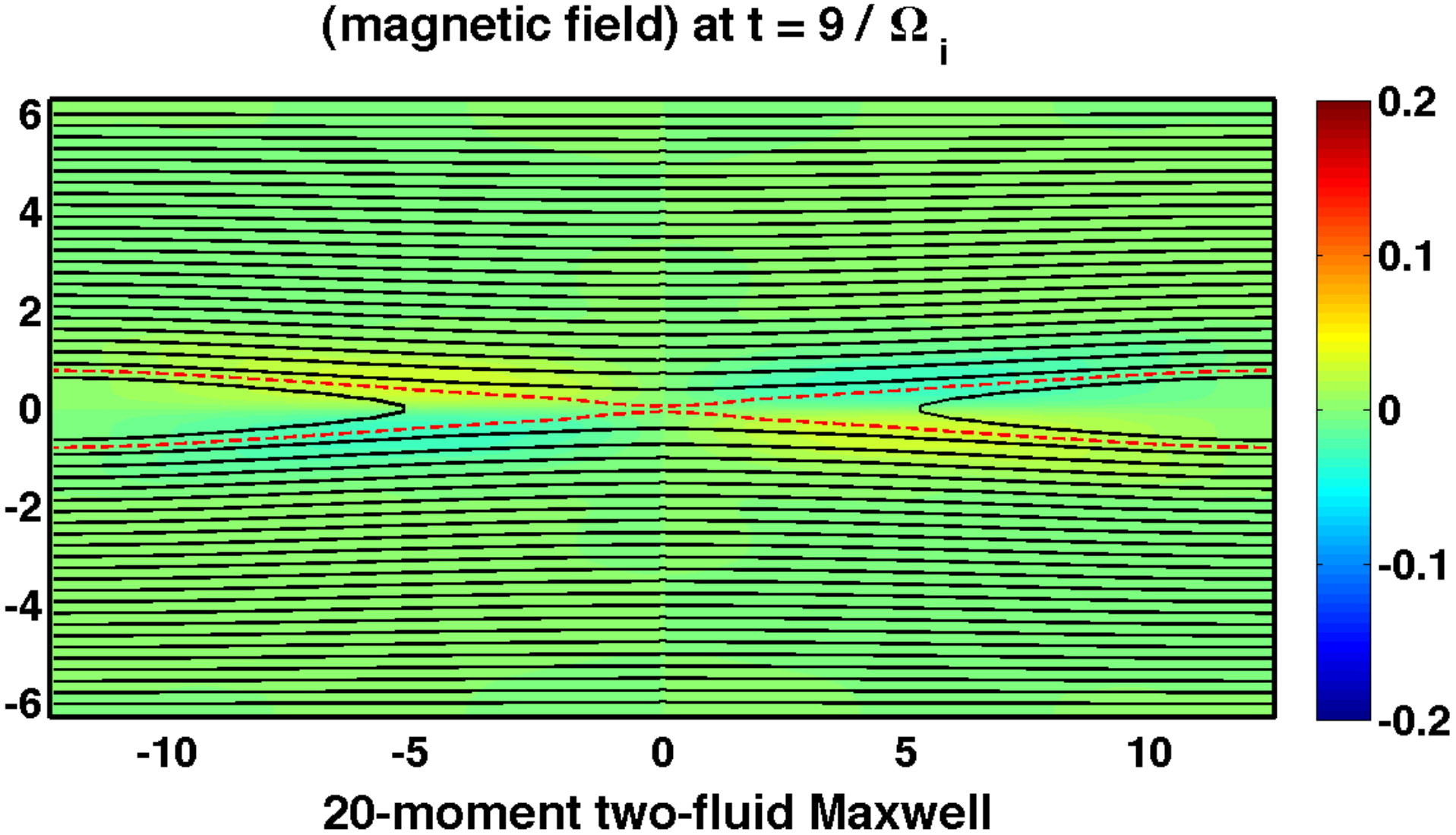
(magnetic field) at t = 9 / Ω i
6
4
2
0
-2
-4
-6
-10
-5
0
5
10
0.2
0.1
0
-0.1
-0.2
20-moment two-fluid Maxwell

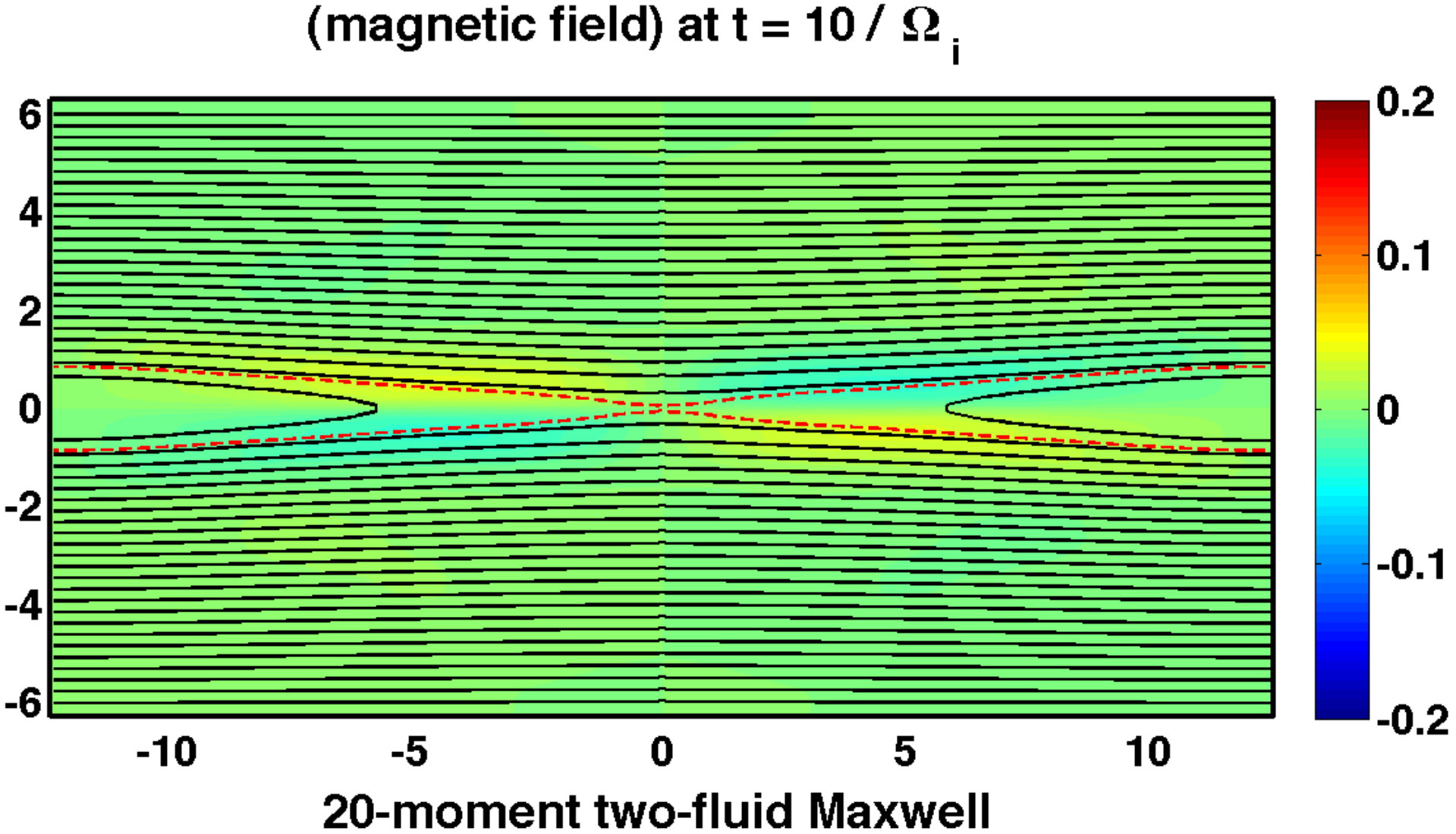
(magnetic field) at t = 10 / Ω i
6
4
2
0
-2
-4
-6
-10
-5
0
5
10
0.2
0.1
0
-0.1
-0.2
20-moment two-fluid Maxwell

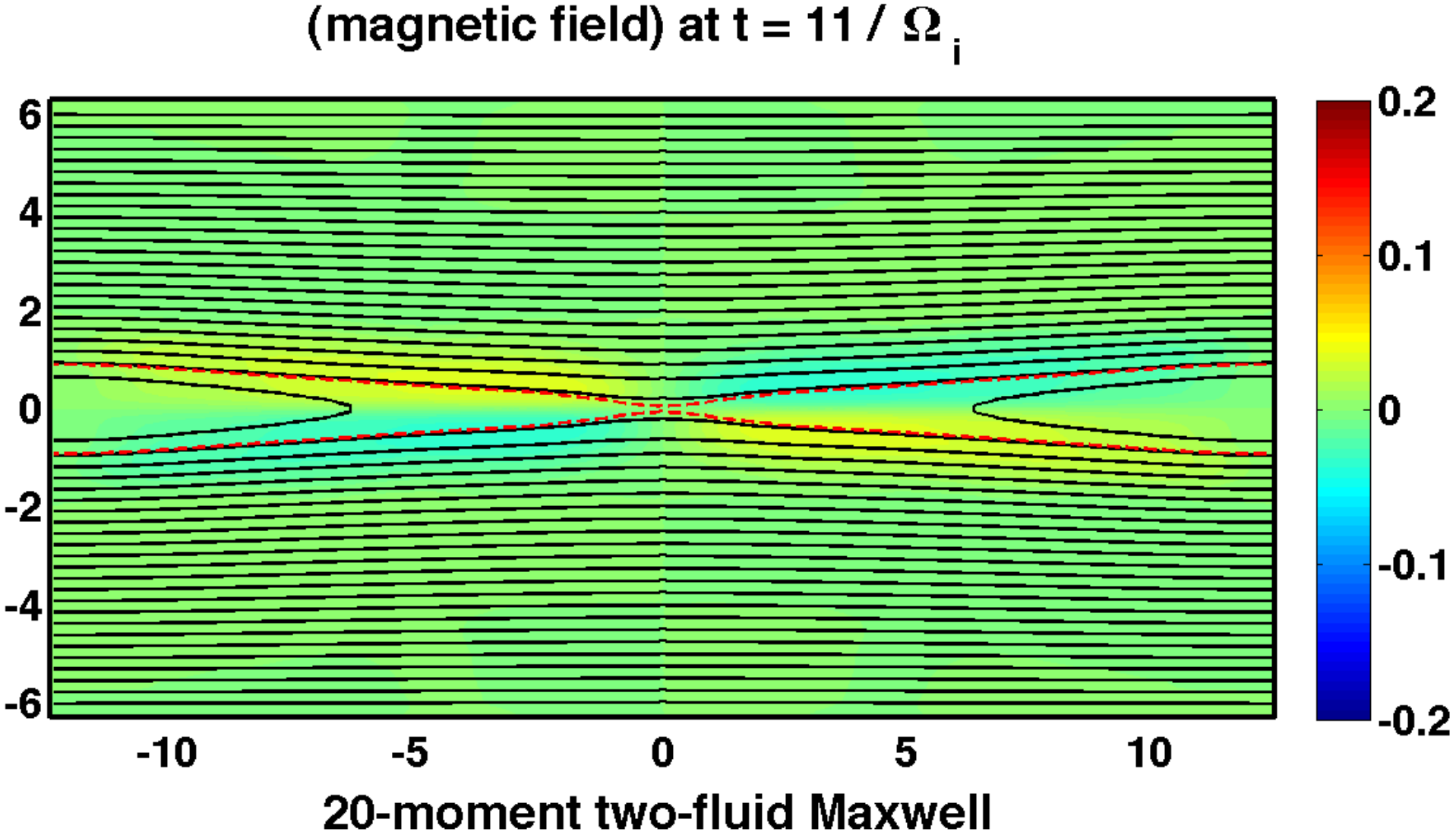
(magnetic field) at t = 11 / Ω i
6
4
2
0
-2
-4
-6
-10
-5
0
5
10
0.2
0.1
0
-0.1
-0.2
20-moment two-fluid Maxwell

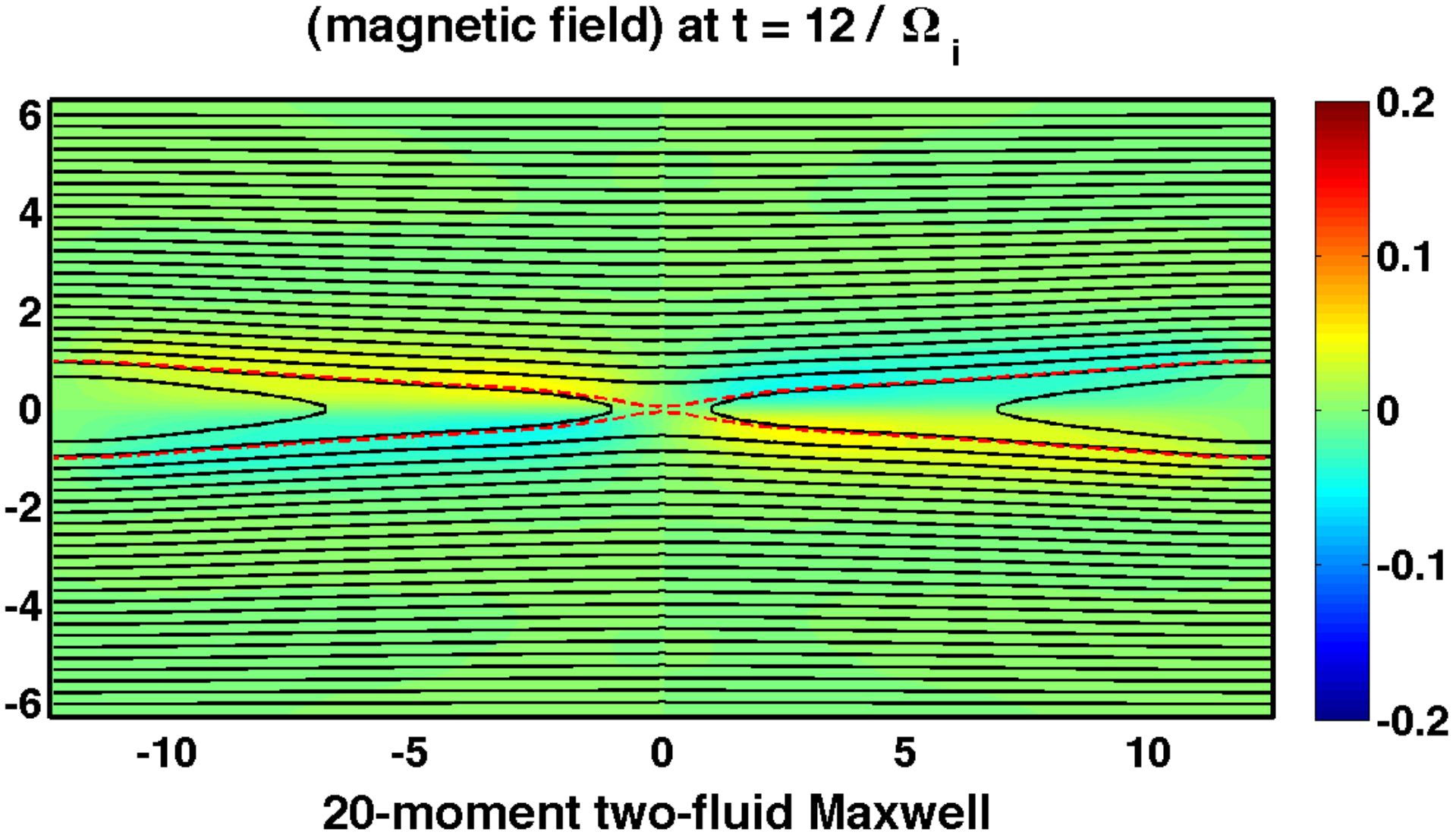
(magnetic field) at t = 12 / Ω i
6
4
2
0
-2
-4
-6
-10
-5
0
5
10
0.2
0.1
0
-0.1
-0.2
20-moment two-fluid Maxwell

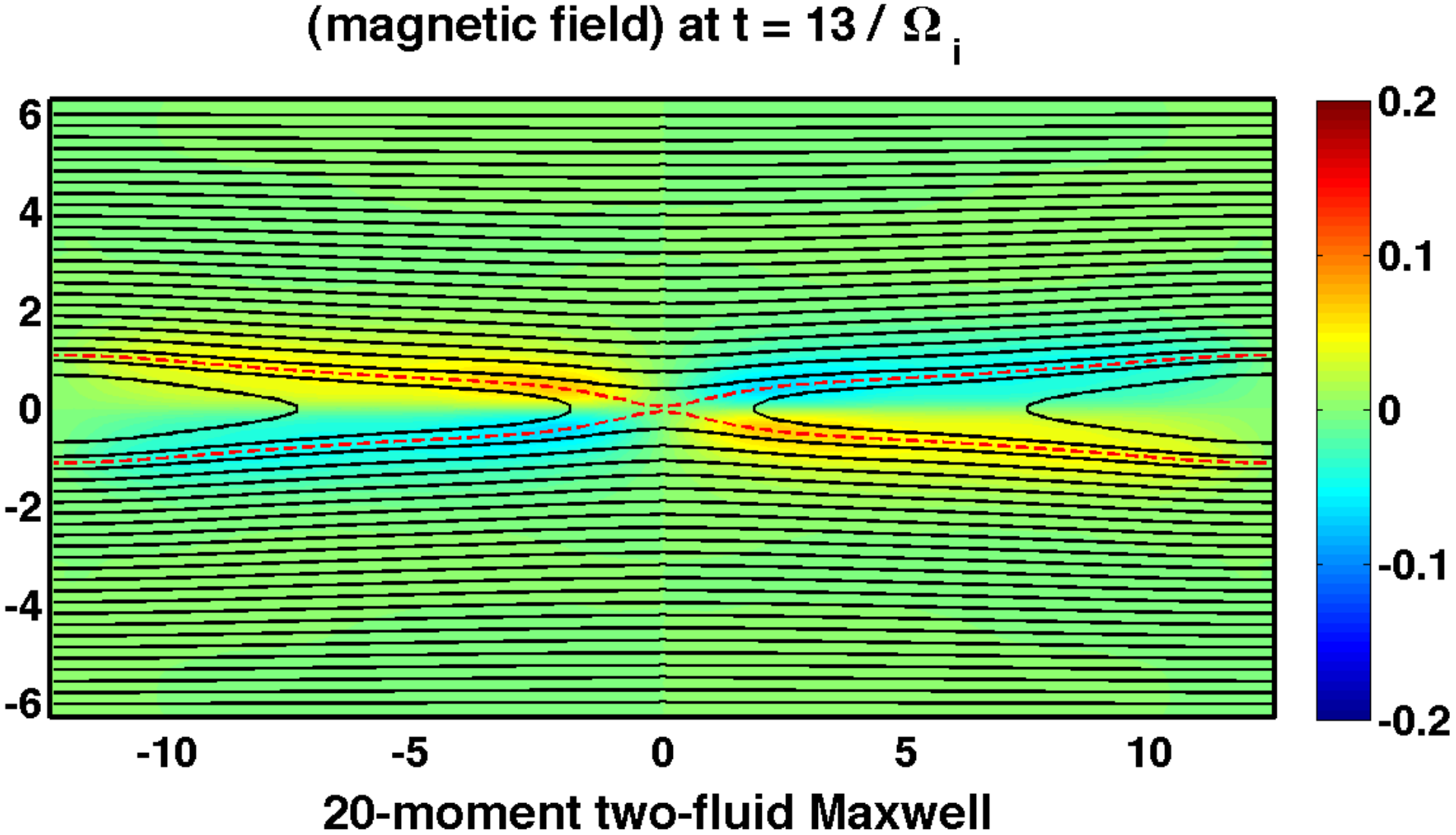
(magnetic field) at t = 13 / Ω i
6
4
2
0
-2
-4
-6
-10
-5
0
5
10
0.2
0.1
0
-0.1
-0.2
20-moment two-fluid Maxwell

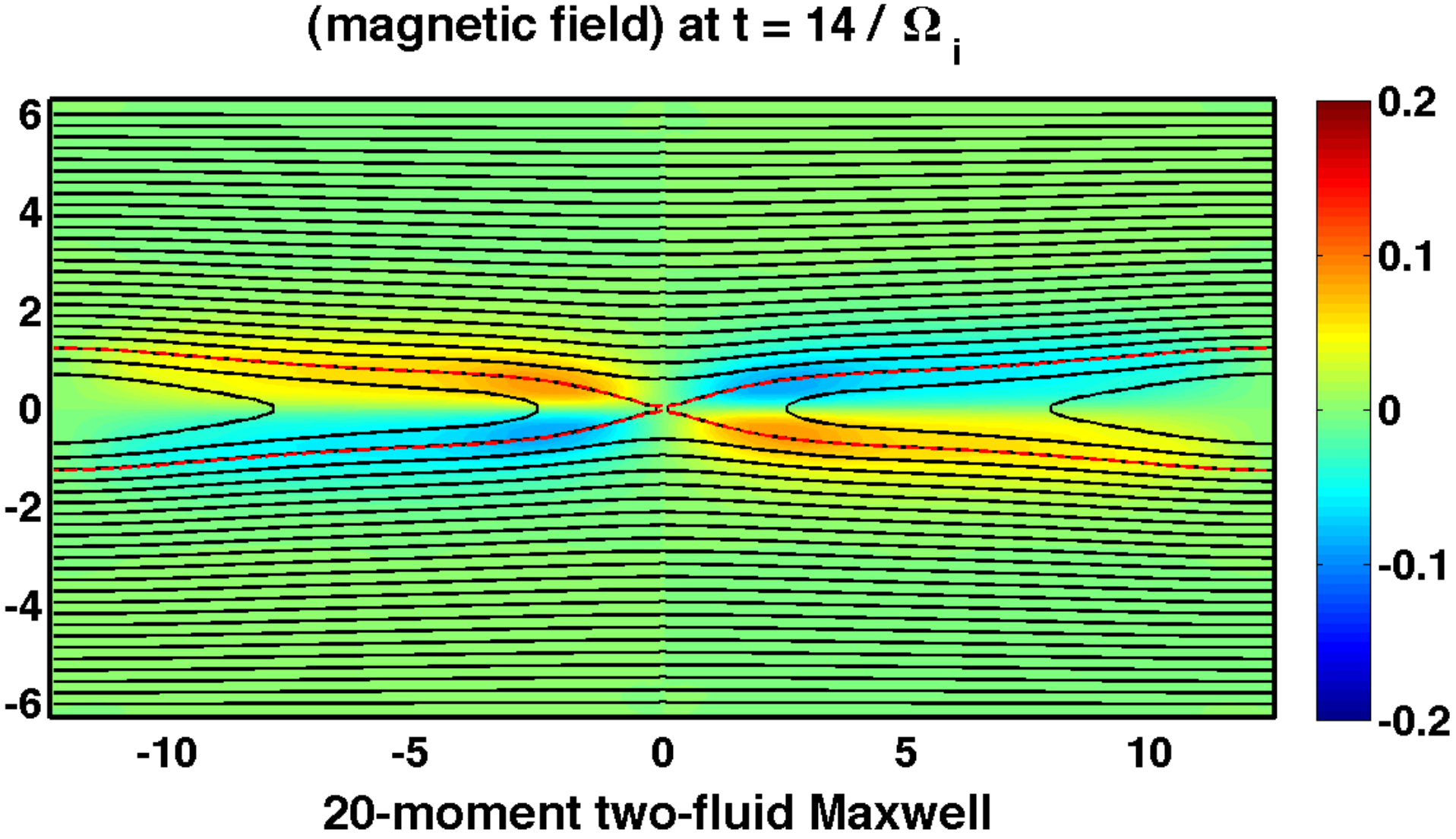
(magnetic field) at t = 14 / Ω i
6
4
2
0
-2
-4
-6
-10
-5
0
5
10
0.2
0.1
0
-0.1
-0.2
20-moment two-fluid Maxwell

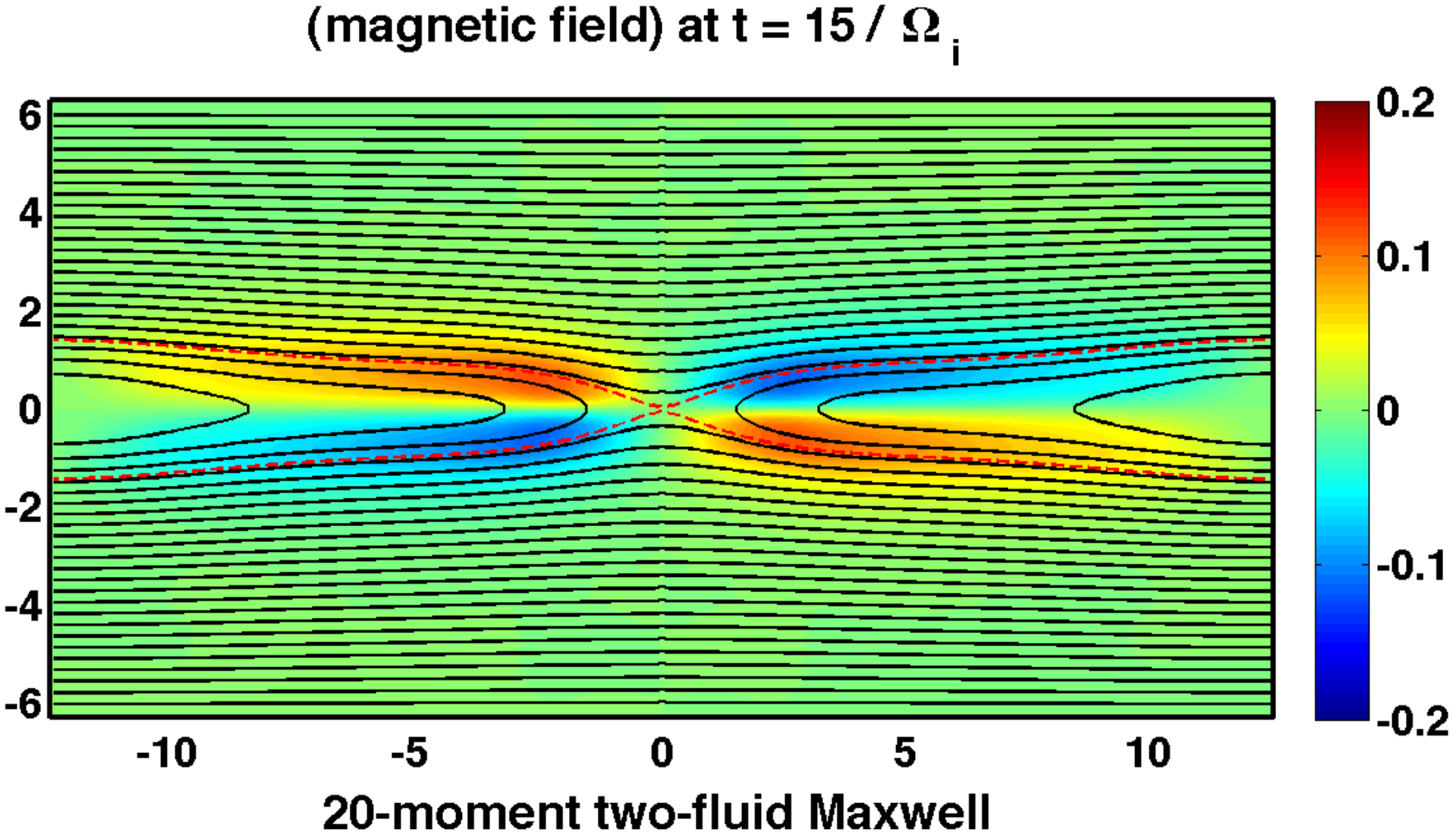
(magnetic field) at t = 15 / Ω i
6
4
2
0
-2
-4
-6
-10
-5
0
5
10
0.2
0.1
0
-0.1
-0.2
20-moment two-fluid Maxwell

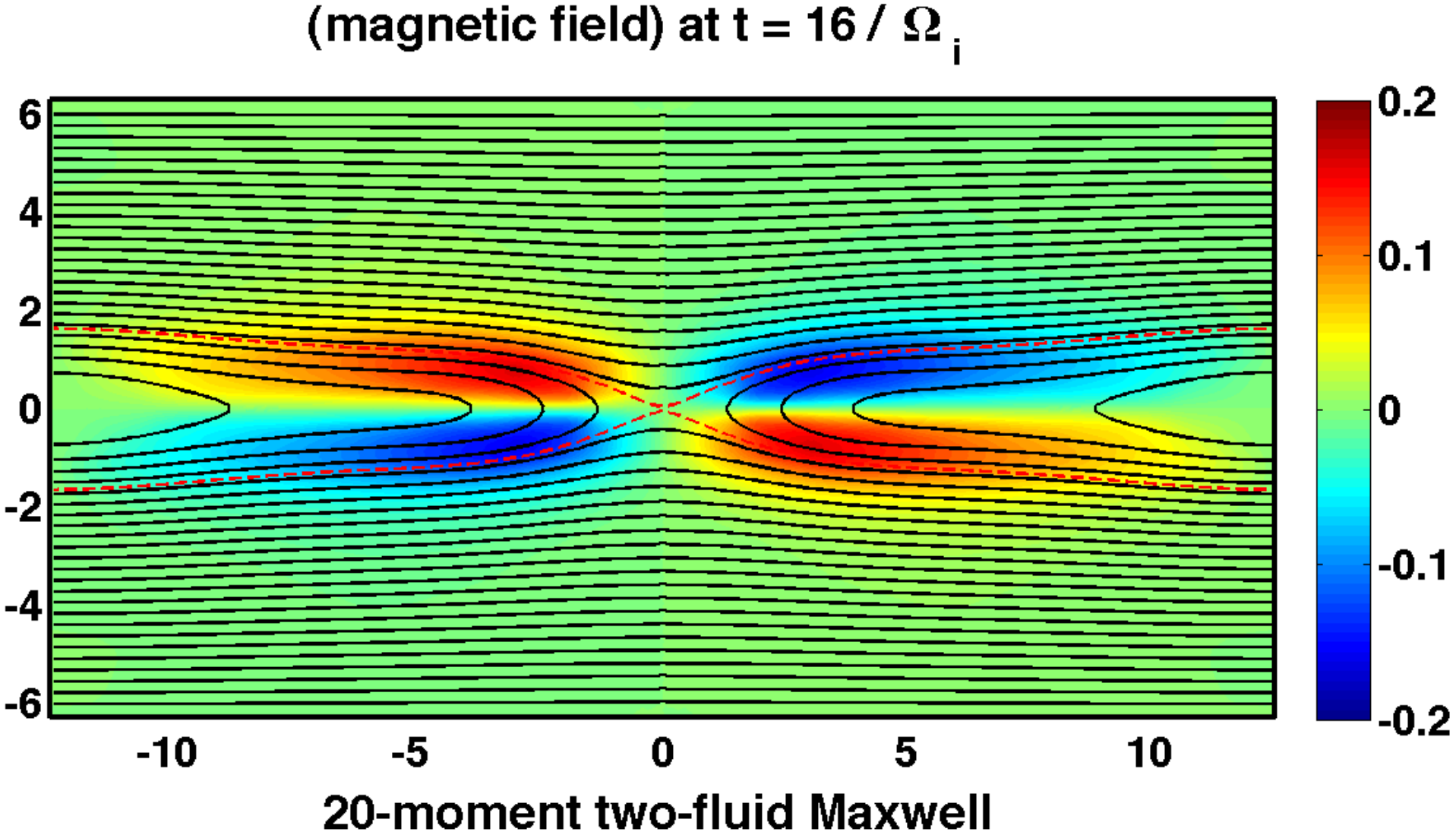
(magnetic field) at t = 16 / Ω i
6
4
2
0
-2
-4
-6
-10
-5
0
5
10
0.2
0.1
0
-0.1
-0.2
20-moment two-fluid Maxwell

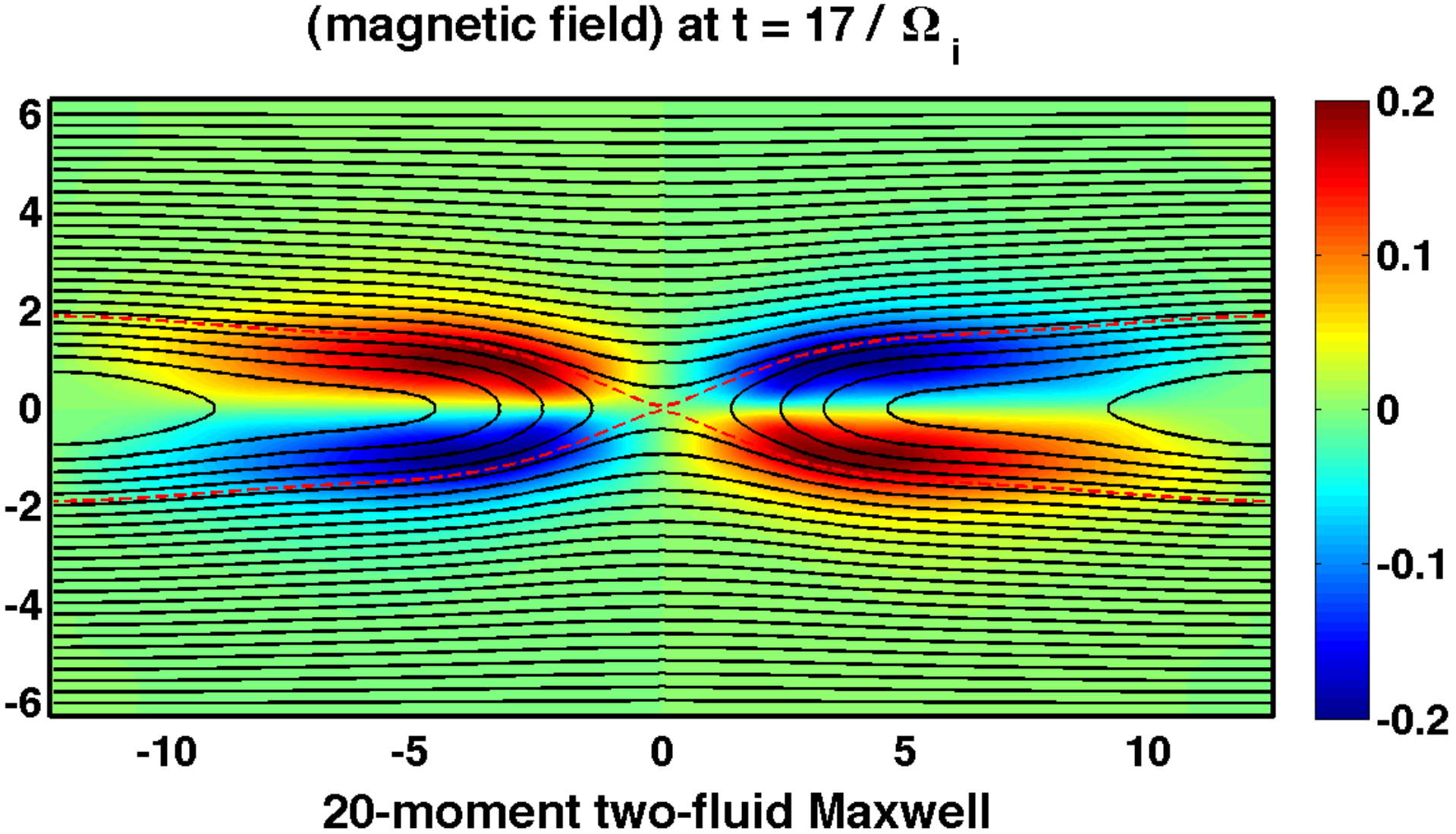
(magnetic field) at t = 17 / Ω i
6
4
2
0
-2
-4
-6
-10
-5
0
5
10
0.2
0.1
0
-0.1
-0.2
20-moment two-fluid Maxwell

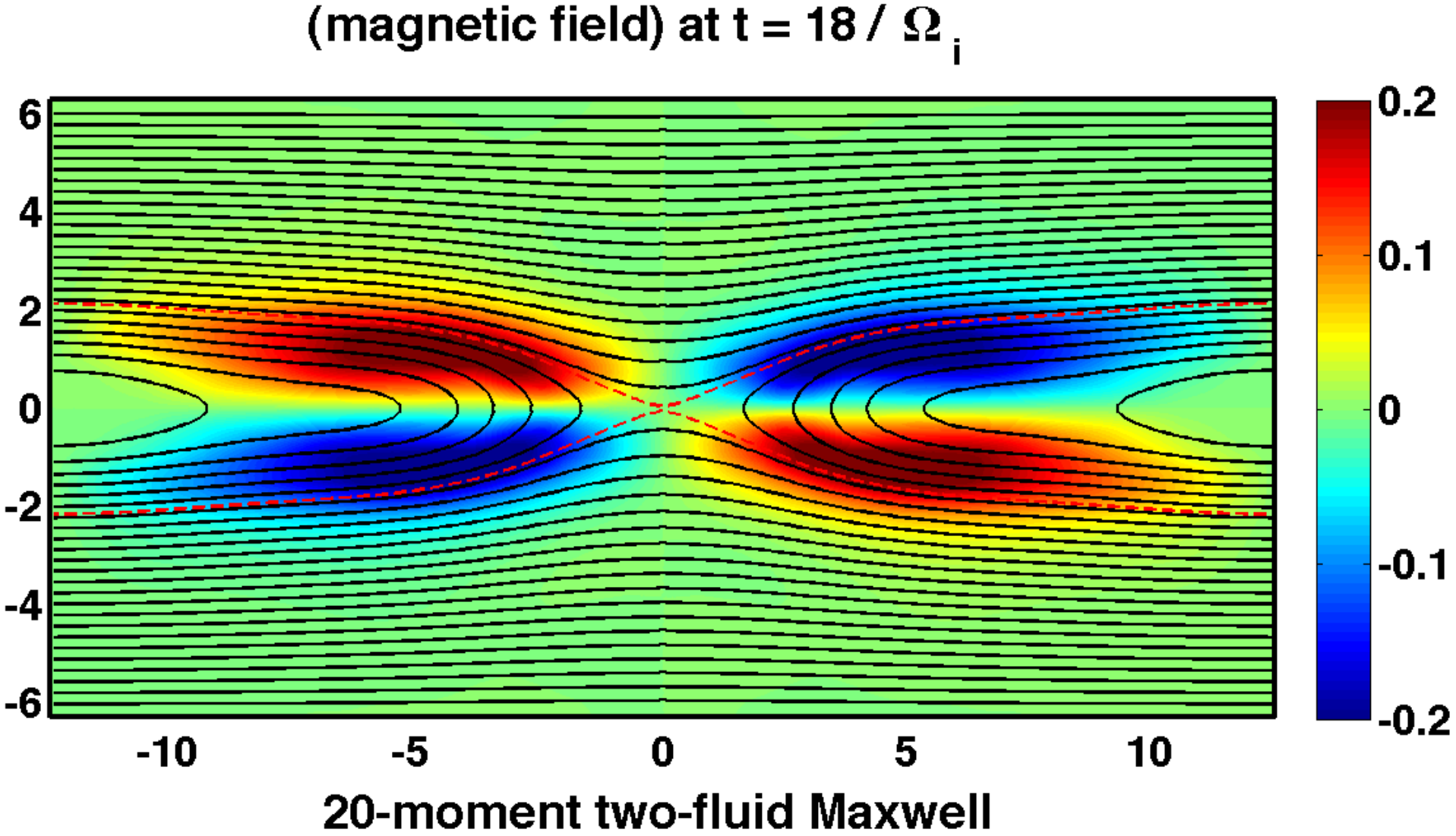
(magnetic field) at t = 18 / Ω i
6
4
2
0
-2
-4
-6
-10
-5
0
5
10
0.2
0.1
0
-0.1
-0.2
20-moment two-fluid Maxwell

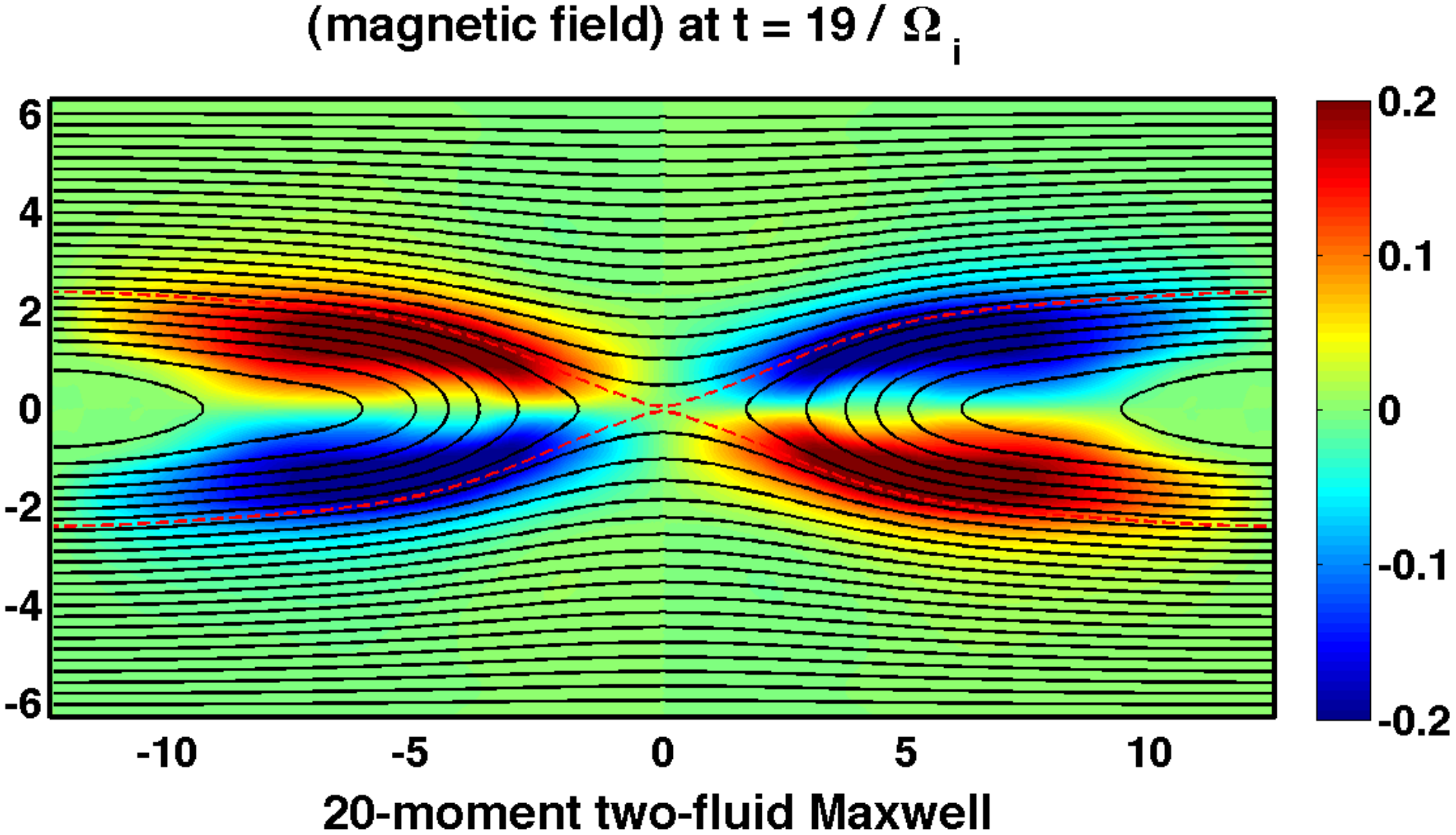
(magnetic field) at t = 19 / Ω i
6
4
2
0
-2
-4
-6
-10
-5
0
5
10
0.2
0.1
0
-0.1
-0.2
20-moment two-fluid Maxwell

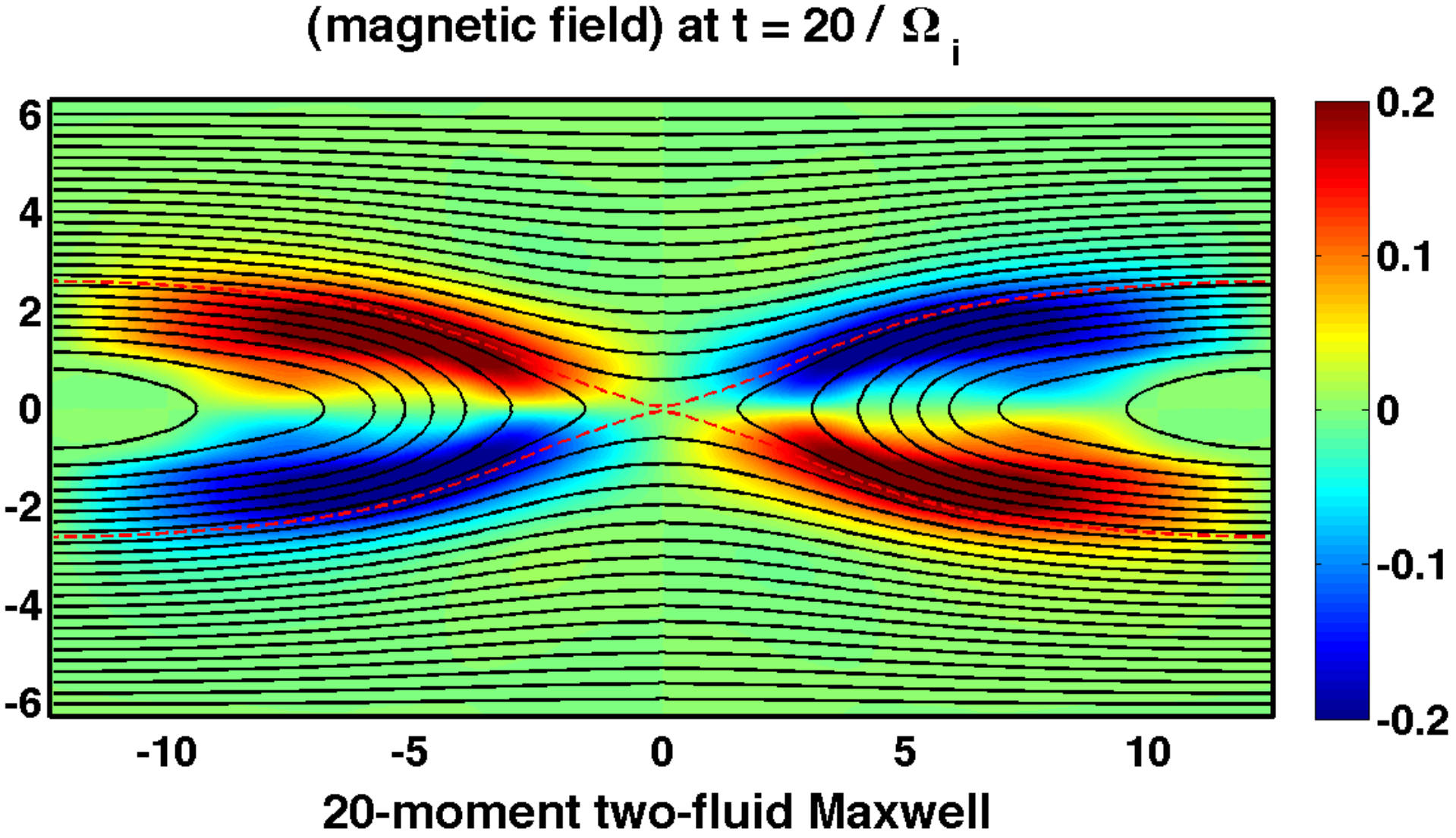
(magnetic field) at t = 20 / Ω i
6
4
2
0
-2
-4
-6
-10
-5
0
5
10
0.2
0.1
0
-0.1
-0.2
20-moment two-fluid Maxwell

Off-diagonal components of electron pressure tensor

The **10-moment** model resolves off-diagonal pressure tensor components well, because it admits viscous stress.

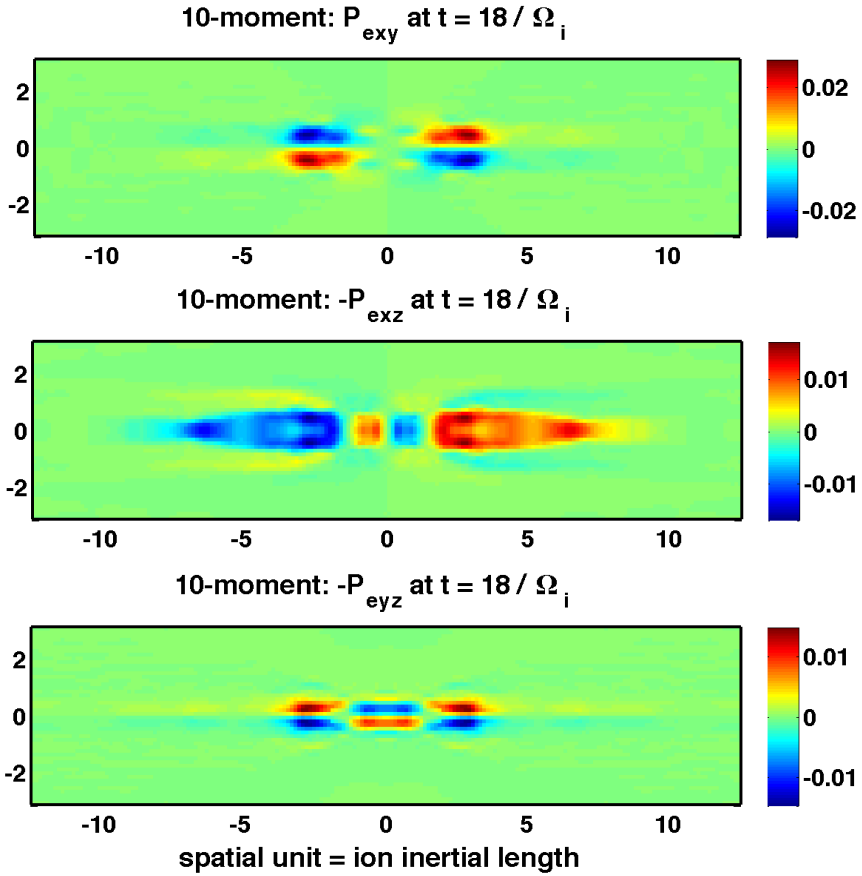

Off-diagonal components of the electron pressure tensor for 10-moment simulation at $\Omega_i t = 18$

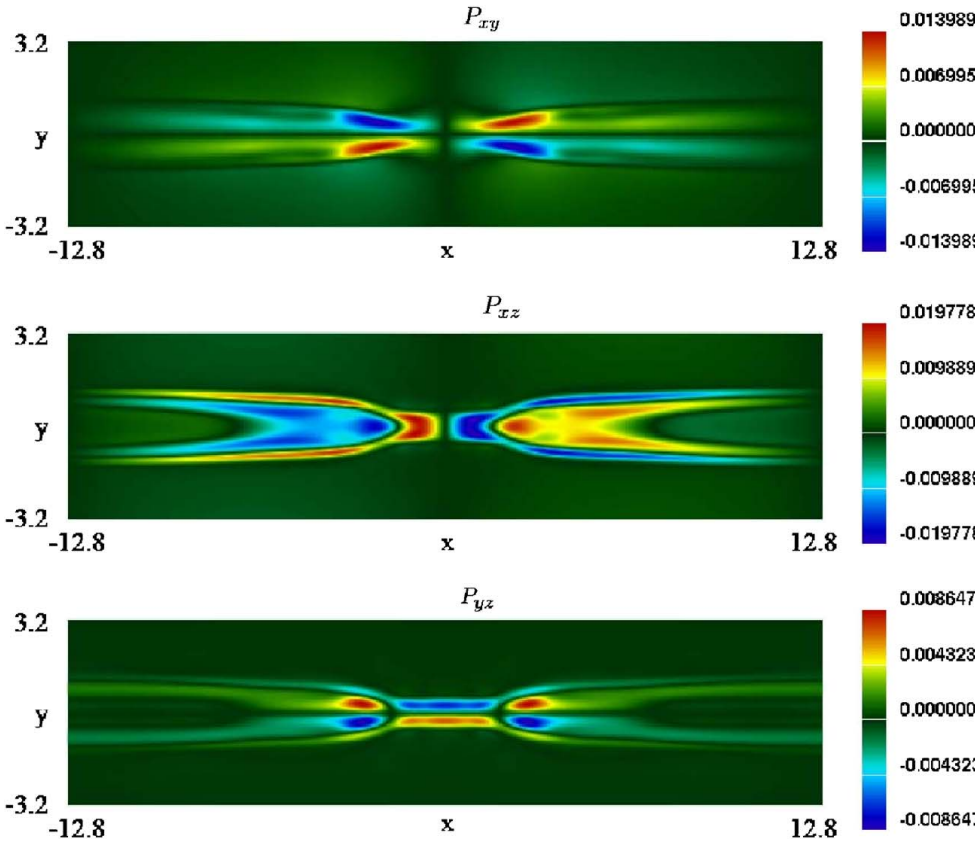

Off-diagonal components of the electron pressure tensor for Vlasov simulation at $\Omega_i t = 17.7$ **[Schmitz-Grauer06]**

Off-diagonal components of electron pressure tensor

The **20-moment** model better resolves the off-diagonal components of the pressure tensor.

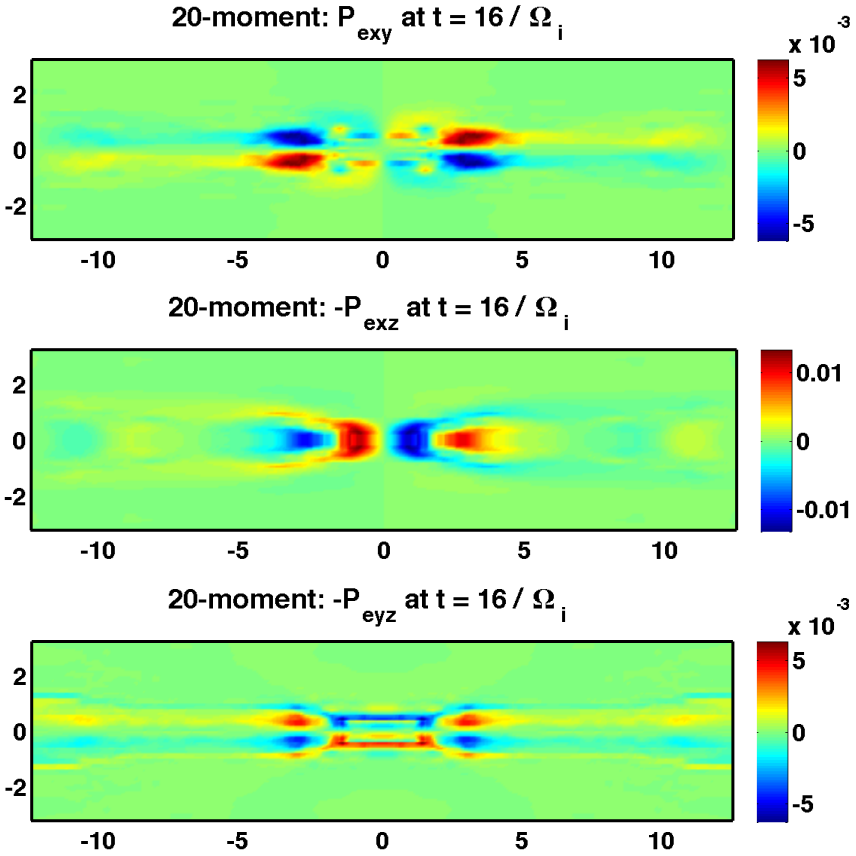

Off-diagonal components of the electron pressure tensor for 20-moment simulation at $\Omega_i t = 16$

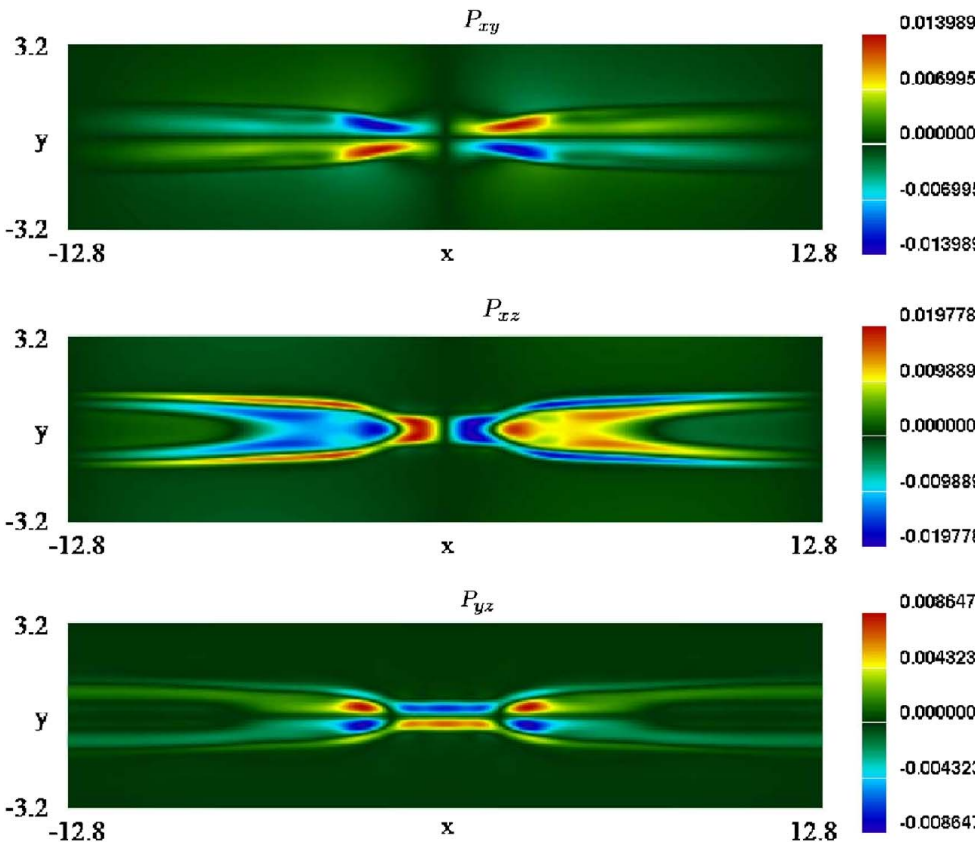

Off-diagonal components of the electron pressure tensor for Vlasov simulation at $\Omega_i t = 17.7$ **[Schmitz-Grauer06]**

Diagonal components of electron pressure tensor

The **10-moment** model resolves the diagonal components of the pressure tensor near the X-point poorly, because it does not admit heat flux.

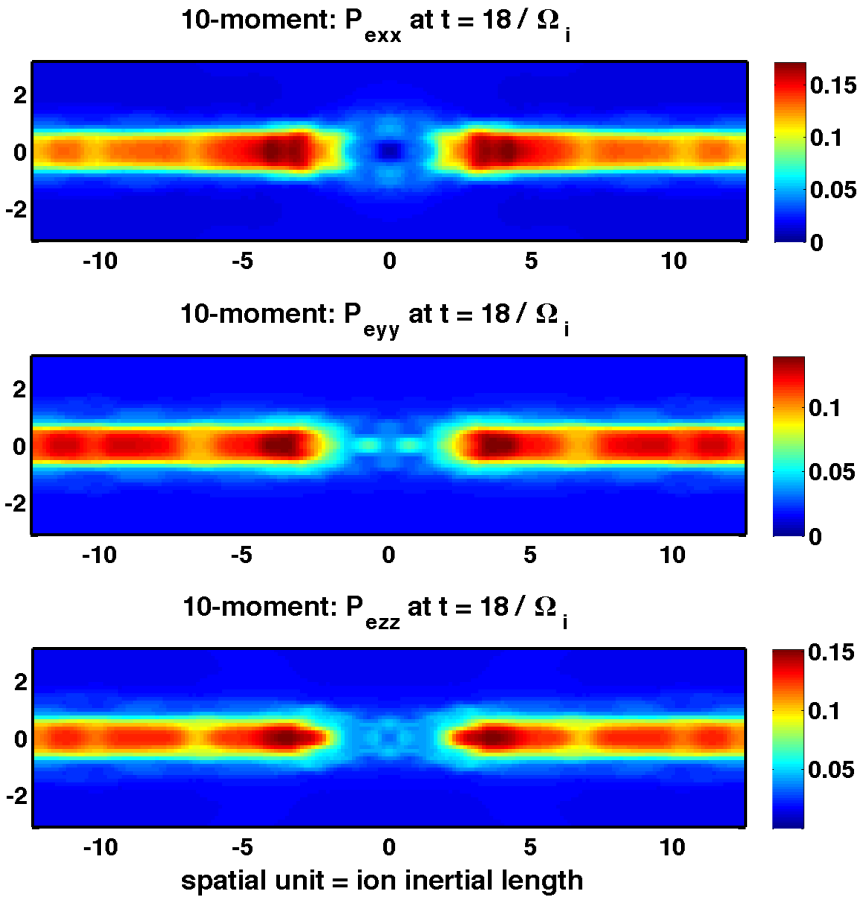

Diagonal components of the electron pressure tensor for 10-moment simulation at $\Omega_i t = 18$

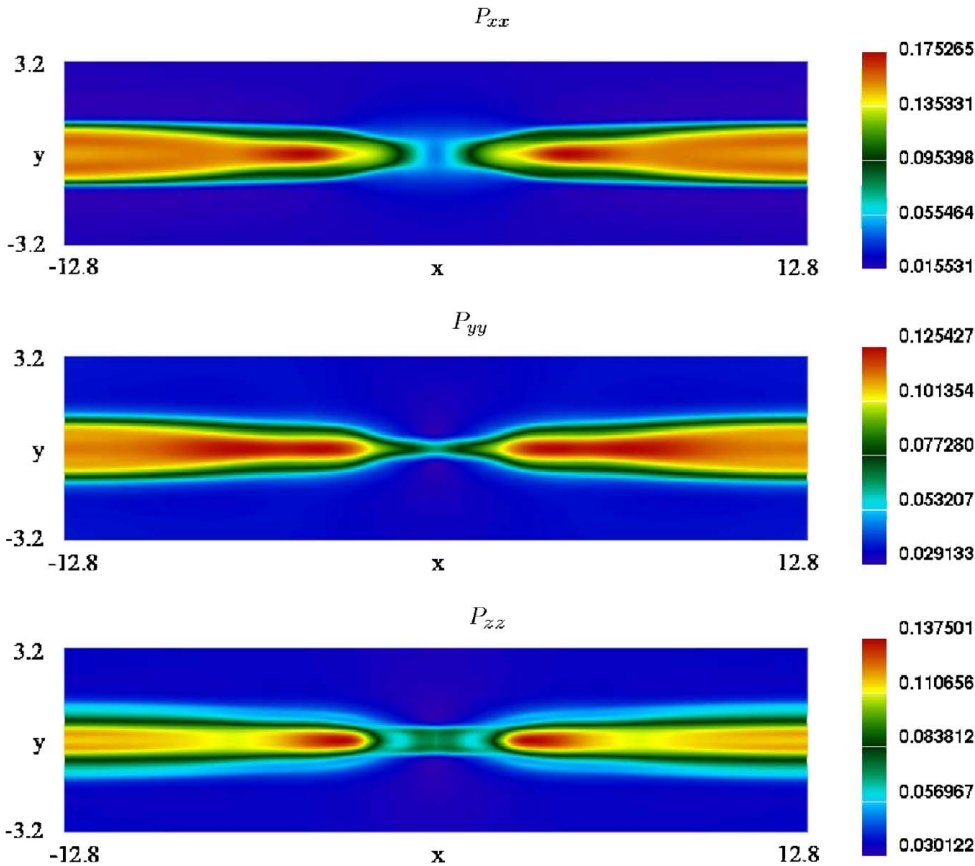

Diagonal components of the electron pressure tensor for Vlasov simulation at $\Omega_i t = 17.7$ **[SchmitzGrauer06]**

Diagonal components of electron pressure tensor

The **20-moment** model resolves the diagonal components of the pressure tensor near the X-point better, because it admits heat flux.

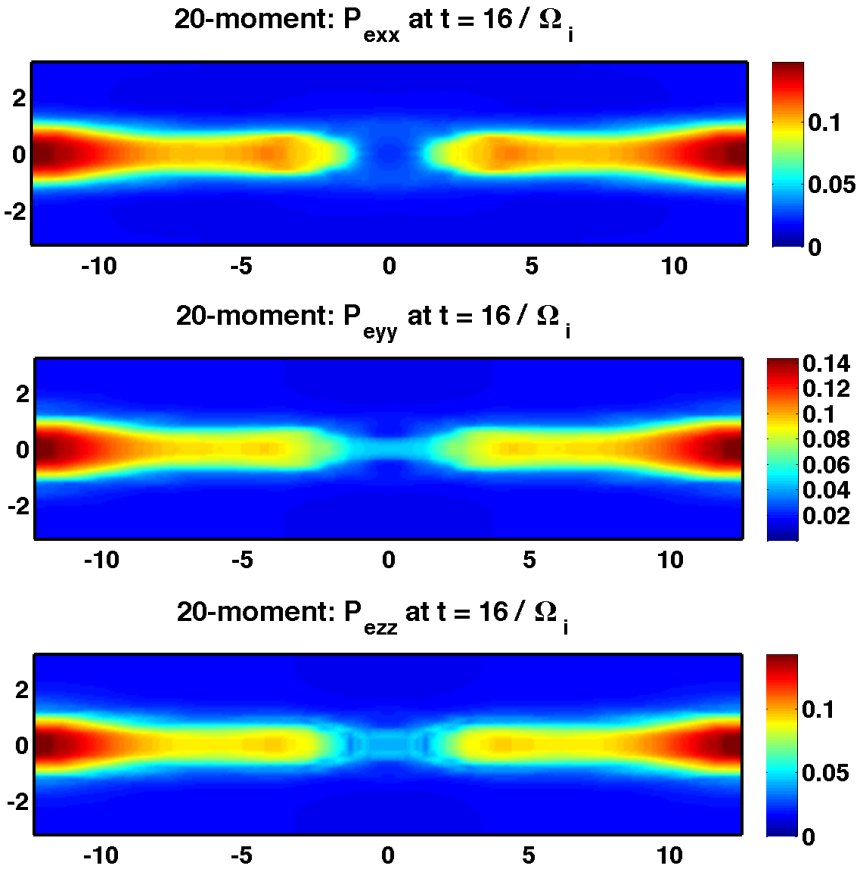

Diagonal components of the electron pressure tensor for 20-moment simulation at $\Omega_i t = 16$

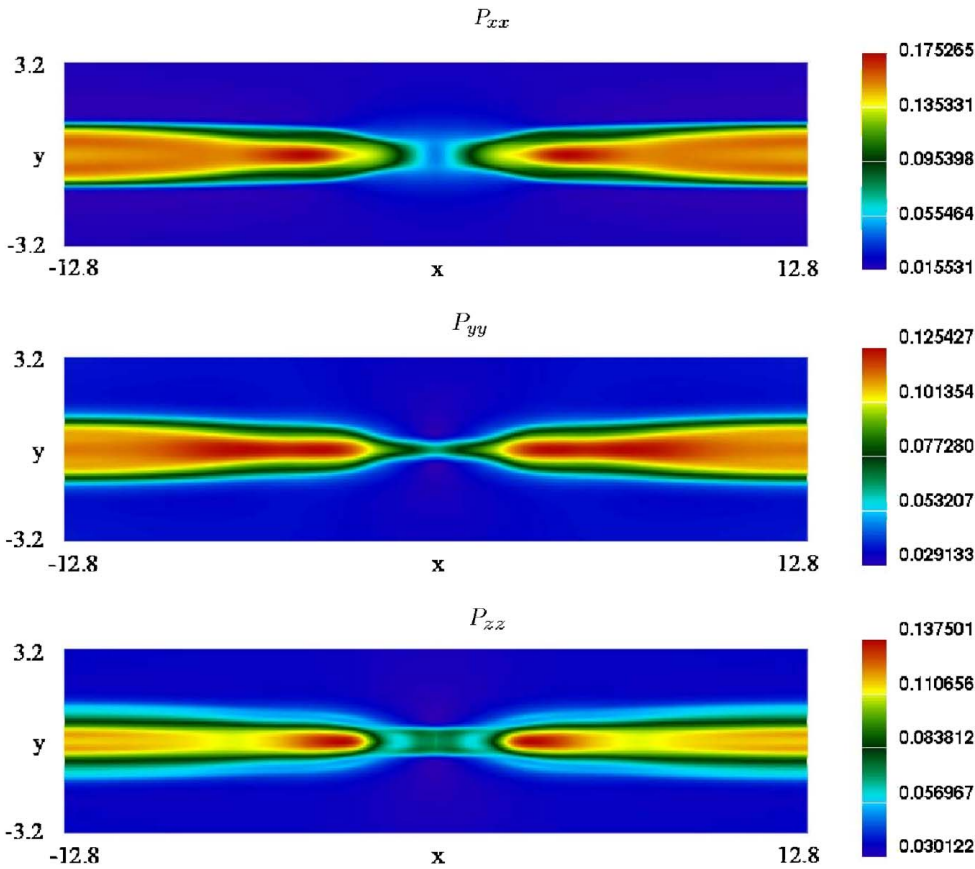

Diagonal components of the electron pressure tensor for Vlasov simulation at $\Omega_i t = 17.7$ **[SchmitzGrauer06]**

Requirements for steady 2D symmetric magnetic reconnection

Consider the simplest reconnection scenario: *steady 2D reconnection symmetric under 180-degree rotation about the X-point.*

Theorem

Reconnection is impossible without viscosity or resistivity.

Argument:

- Rate of reconnection is the electric field strength at the X-point.
- Electric field strength at the X-point is resistive electric field plus viscous electric field.

Theorem (Jo11)

Reconnection is impossible for any conservative model for which heat flux is zero.

Argument:

- Steady reconnection requires entropy production near the X-point (via resistivity or viscosity).
- The X-point is a stagnation point.
- Without heat flux, heat accumulates at the X-point without bound.

Observation: in kinetic simulations, fast reconnection is supported by viscosity, not resistivity.

Conclusion: we need heat flux and viscosity in a fluid model of fast magnetic reconnection.

Performance summary of fluid models

Performance of hyperbolic fluid models relative to kinetic simulations:

- 5-moment
  - *Success:* rate of reconnection is qualitatively correct.
  - *Reason for success:* reconnection wants to happen, and the inertial term provides a mechanism.
  - *Failure:* reconnection is supported by inertial term rather than pressure term.
  - *Reason for failure:* lack of viscosity forces current to ramp at the X-point until mitigated by numerical resistivity. [Jo11]
- 10-moment [Jo11]:
  - *Success:* pressure tensor supports reconnection
    - model shows reasonable resolution of off-diagonal components of electron pressure tensor. [JoRo10].
    - reconnection is insensitive to collision period τ_s
    - reconnection is robust and reliable if $\tau_s \neq \infty$ is used to damp oscillations in deviatoric stress [Jo11]
  - *Reason for success:* the model admits viscosity.
  - *Failure:* diagonal components of pressure tensor are poorly resolved near X-point
  - *Reason for failure:* lack of heat flux forces entropy and pressure anisotropy to ramp at the X-point. Instability eventually kicks in. [Jo11]
- 20-moment:
  - *Success:* diagonal components of electron pressure tensor are resolved near X-point.
  - *Reason for success:* the model admits heat flux to relieve temperature pile-up.
  - *Issue:* need for positivity limiting and instability are seen at late times.
  - *What to do about it:*
    - A generic framework for positivity limiting is developed in [JoRo13].
    - The GEM problem is unstable to secondary plasmoid formation, so convergence becomes unfeasible for any accurate model at late times.
    - For stable steady reconnection an implicit method is called for.

References

[Brown96] Shawn Lee Brown. Approximate Riemann solvers for moment models of dilute gases. PhD thesis, University of Michigan (1996).

[GEM01] J. Birn, J. Drake, M. Shay, B. Rogers, R. Denton, M. Hesse, M. Kuznetsova, Z. Ma, A. Bhattacharjee, A. Otto, and P. Pritchett. Geospace environmental modeling (GEM) magnetic reconnection challenge. *Journal of Geophysical Research — Space Physics*, 106:3715–3719, 2001.

[GrothGRB94] Clinton P. T. Groth, Tamas I. Gombosi, Philip L. Roe, and Shawn L. Brown, Gaussian-based moment-method closures for the solution of the Boltzmann equation. *Proceedings of the Fifth International Conference on Hyperbolic Problems. Theory, Numerics, Applications*. University of New York at Stony Brook, Stony Brook, New York, USA, 1994, World Scientific, New Jersey, pp. 339–346.

[Grad49] Harold Grad. On the Kinetic Theory of Rarefied Gases. *Commun. Pure Appl. Math.*, Vol. 2, pp. 331–407.

[GrothGRB03] C.P.T. Groth, T.I. Gombosi, P.L. Roe, and S.L. Brown. A Gaussian-based closure for rarefied gases: derivation, moment equations, and wave structure. Unpublished paper written in 2003 and obtained from Groth.

[Hakim06] A. Hakim. Extended MHD modelling with the ten-moment equations. *Journal of Fusion Energy*, 27 (2008).

[HaLoSh06] A. Hakim, J. Loverich, and U. Shumlak. A high-resolution wave propagation scheme for ideal two-fluid plasma equations. *J. Comp. Phys.*, 219 (2006), pp. 418–442.

[Jo11] E.A. Johnson, Gaussian-Moment Relaxation Closures for Verifiable Numerical Simulation of Fast Magnetic Reconnection in Plasma. PhD thesis, UW–Madison, 2011

[JoRo10] E. A. Johnson and J. A. Rossmanith, Ten-moment two-fluid plasma model agrees well with PIC/Vlasov in GEM problem. *'proceedings for HYP2010*, November 2010.

[JoRo13] E. A. Johnson and J. A. Rossmanith, Outflow Positivity Limiting for Hyperbolic Conservation Laws. Part I: Framework and Recipe. `http://arxiv.org/abs/1212.4695`.

[LoHaSh11] J. Loverich, A. Hakim, and U. Shumlak A discontinuous Galerkin method for ideal two-fluid plasma equations. *Commun. Comput. Phys.*, 9 (2011), pp. 240–268.

[SchmitzGrauer06] H. Schmitz and R. Grauer. Darwin-Vlasov simulations of magnetised plasmas. *J. Comp. Phys.*, 214 (2006), pp. 738–756.